Microzooplankton diversity and potential role in carbon cycling of contrasting Southern Ocean productivity regimes

Urania Christaki, Dimitra-Ioli Skouroliakou, Alice Delegrange, Solène Irion, Lucie Courcot, Ludwig Jardillier, Ingrid Sassenhagen

Journal of Marine Systems 219 (2021) 103531

Contents lists available at ScienceDirect

Journal of Marine Systems

journal homepage: www.elsevier.com/locate/jmarsys

Microzooplankton diversity and potential role in carbon cycling of contrasting Southern Ocean productivity regimes

Urania Christaki [a,*], Ioli-Dimitra Skouroliakou [a], Alice Delegrange [a,b], Solène Irion [a], Lucie Courcot [a], Ludwig Jardillier [c], Ingrid Sassenhagen [a,d]

[a] Univ. Littoral Côte d'Opale ULCO, CNRS, Univ. Lille, UMR 8187, LOG, Laboratoire d'Océanologie et de Géosciences, 62930 Wimereux, France
[b] Institut national supérieur du professorat et de l'éducation, Académie de Lille – Hauts de France, 59658 Villeneuve d'Ascq, France
[c] Université Paris-Saclay, CNRS, AgroParisTech, Ecologie Systématique Evolution, Orsay, France
[d] Department of Ecology and Genetics/Limnology, Uppsala University, Norbyvägen 18D, 75236 Uppsala, Sweden

ARTICLE INFO

Keywords:
Dinoflagellates
Ciliates
Microscopy
Metabarcoding
Dilution experiments
Southern Ocean
Microzooplankton
Diversity

ABSTRACT

Microzooplankton play an important role in aquatic food webs through their multiple interactions with other organisms and their impact on carbon export. They are major predators of phytoplankton and bacteria while being preyed on by higher trophic levels. Microzooplankton diversity (Dinoflagellates, DIN and Ciliates, CIL), community structure, interaction with phytoplankton and its potential in channeling carbon to higher trophic levels were studied in contrasting productivity regimes (off- and on-plateau, the latter been naturally fertilized by iron) around the Kerguelen islands in the Southern Ocean (SO). DIN and CIL diversity was sampled in late summer (February–March 2018; project MOBYDICK) and at the onset-of the bloom (KEOPS2 cruise), and assessed by Illumina sequencing of 18S rDNA amplicons and microscopic observations. The diversity obtained by the two approaches could be compared at a relatively high taxonomic level (i.e., often to family level). In particular for DIN, relative abundances and ranking of dominant taxa differed between sequencing and microscopy observations. CIL were always recorded at considerably lower abundances than DIN, the median of their abundances across stations and seasons being 350 and 1370 cells L^{-1}, respectively. During late summer, DIN and CIL biomasses were about 1.5 times higher on- than in off-plateau waters, while community composition was spatially similar. The most abundant DIN at all stations and during both seasons were small *Gymnodinium* (<20 μm). During late summer, ciliates *Lohmaniella oviformis* (<20 μm) and *Cymatocylis antarctica* (20-40 μm) dominated on- and off-plateau, respectively. Dilution experiments suggested significant grazing of microzooplankton on phytoplankton as phytoplankton net growth (k) was lower than microzooplankton grazing (g) at all stations (mean k = 0.16 ± 0.05 d^{-1}, g = 0.36 ± 0.09 d^{-1}) in late summer. Despite having great potential as a phytoplankton grazer, microzooplankton occurred at low biomass and showed little temporal variability, suggesting that it was controlled by copepod predation. Microzooplankton is a key component of the SO as an intermediate trophic level mediating carbon transfer from primary producers to higher trophic levels.

1. Introduction

Dinoflagellates (DIN) and ciliates (CIL) represent the most abundant microzooplankton groups in planktonic food webs, where they play a pivotal role as phytoplankton consumers, food source for mesozooplankton and contributors to nutrient remineralization (e.g., Calbet and Landry, 2004; Irigoien et al., 2005; Sherr and Sherr, 2007, 2009; Caron and Hutchins, 2013; Steinberg and Landry, 2017 and references therein). The proportion of carbon produced by the phytoplankton that is ingested by microzooplankton is highly variable and can exceed mesozooplankton consumption (e.g., Calbet and Landry, 2004; Schmoker et al., 2013; Menden-Deuer et al., 2018). Microzooplankton is able to closely track phytoplankton temporal dynamics because they overall share similar growth rates. Blooms, thus occur when particular phytoplankton taxa successfully escape microzooplankton control (Irigoien et al., 2005; Sherr and Sherr, 2009). At a global scale, predatory protists and phytoplankton biomass display a curvilinear relationship and the plateau observed at about 50 μg C L^{-1} for phytoplankton has

* Corresponding author.
E-mail address: urania.christaki@univ-littoral.fr (U. Christaki).

https://doi.org/10.1016/j.jmarsys.2021.103531
Received 29 June 2020; Received in revised form 25 February 2021; Accepted 27 February 2021
Available online 7 April 2021

been attributed to predation by mesozooplankton (Irigoien et al., 2005). In fact, mesozooplankton preferentially grazes on microzooplankton (e.g., Stoecker and Capuzzo, 1990; Kiørboe and Visser, 1999; Calbet and Saiz, 2005; Vargas and González, 2004; Campbell et al., 2009; Sherr and Sherr, 2009), releasing predation pressure on phytoplankton and favoring its blooming capacity (e.g., Grattepanche et al., 2011a). Due to the central position of microzooplankton in aquatic food webs and the direct interaction with primary producers, any change in community structure and activity can have marked implications for multiple trophic levels and carbon export. Such changes in carbon export are expected in the future, as modeling studies suggest that ocean warming will enhance loss of primary production to microzooplankton herbivory in chlorophyll rich waters (Chen et al., 2012). Trophic transfer of carbon produced by phytoplankton through microzooplankton rather than directly via mesozooplankton predation would result in lower C-export (Hall and Safi, 2001; Smetacek et al., 2004). Despite several centuries of studies on protists, untangling the impact on carbon transfer of heterotrophic protists in plankton communities remains challenging due to their fragility, lack of direct methods to accurately measure their growth rate, and time-consuming identification and counting (reviewed in Caron et al., 2009, 2012; Caron and Hutchins, 2013).

In the Southern Ocean (SO), diatoms and haptophytes are usually identified as the major primary producers and their diversity and role in the C-cycle have been described in detail in previous studies (e.g., Smetacek et al., 2004; Poulton et al., 2007; Armand et al., 2008; Quéguiner, 2013; Wolf et al., 2014, Lasbleiz et al., 2016, Irion et al., 2020 among many others). By contrast, microbial heterotrophs and, in particular, phytoplankton predators, have been far less investigated (Caron et al., 2000; Hall and Safi, 2001; Saito et al., 2005; Henjes et al., 2007; Christaki et al., 2008; Poulton et al., 2007; Christaki et al., 2015; Morison and Menden-Deuer, 2018 and references therein). In the SO, Kerguelen and Crozet islands are characterized by iron enrichment of surface waters. This results in large phytoplankton blooms in these waters that contrast with the surrounding HNLC (High Nutrients Low Chlorophyll) conditions (Blain et al., 2007; Pollard et al., 2007, 2009). The rare studies that have provided information on microzooplankton community structure in the Crozet and Kerguelen areas reported a prevalence of DIN over CIL biomass (Poulton et al., 2007; Christaki et al., 2015). Microzooplankton were identified as a major consumer of phytoplankton during the onset and decline of Kerguelen blooms (Brussaard et al., 2008; Christaki et al., 2015) and an important player in iron regeneration (Sarthou et al., 2008).

The present study was realized in the framework of the MOBYDICK project (Marine Ecosystem Biodiversity and Dynamics of Carbon around Kerguelen: an integrated view). MOBYDICK's aim was to trace C from its biological fixation and cycling within and across trophic levels at surface, as well as its export to depth under different productivity regimes of the Southern Ocean after the phytoplankton bloom, in late summer. The objective of this study was to provide information about the diversity and the community structure of microzooplankton (DIN and CIL) in relation to phytoplankton communities and to estimate their potential capacity for channeling carbon to higher trophic levels. The results obtained during the post-bloom period (MOBYDICK cruise) are discussed here along with observations from the onset of a previous bloom (KEOPS2 cruise).

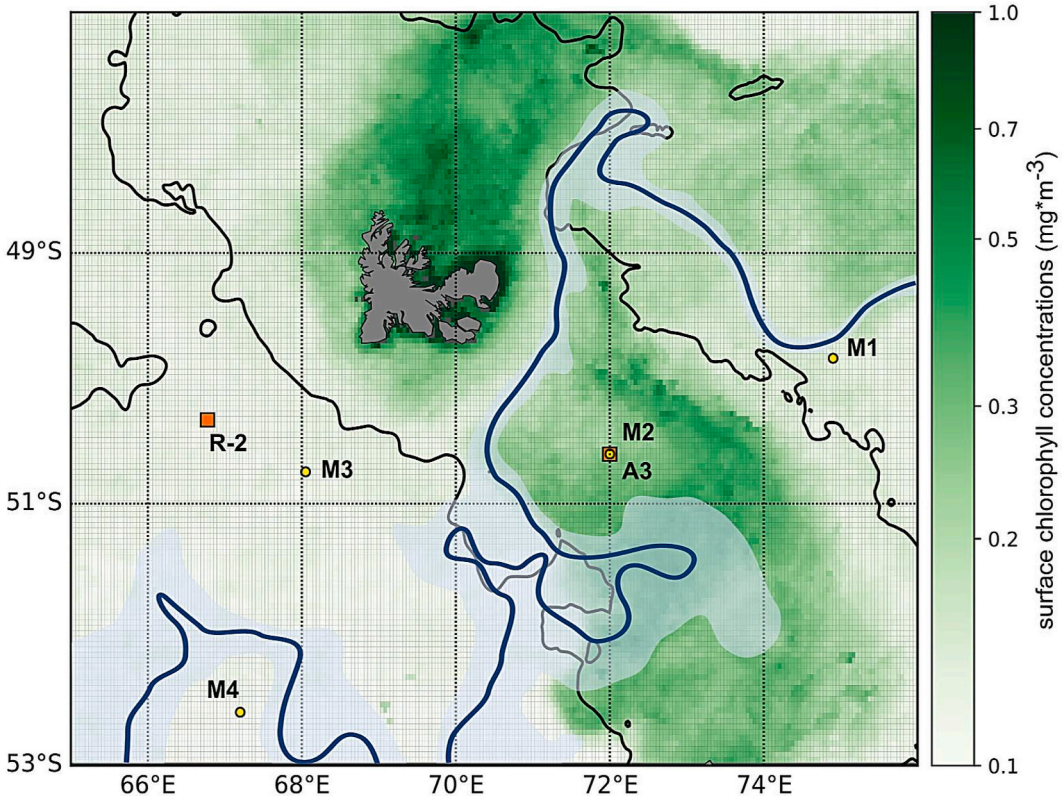

Fig. 1. Location of stations Surface Chlorophyll *a* concentrations during MOBYDICK are the monthly means for March 2018 at a resolution of 4 km (Copernicus Marine Service, http://marine.copernicus.eu/). The black lines denote 1000 m bathymetry. The approximate position of the highly dynamic polar front (PF, blue line) during February–March 2018 was also drawn according to Pauthenet et al. (2018), gray zone around the polar front indicates variations in its trajectory. The position of the on-plateau A3 and reference HNLC R stations sampled during early spring (KEOPS2 cruise, October–November 2011) are also indicated on this map. KEOPS2 station A3 was named M2 during the MOBYDICK cruise and has the same coordinates. (For interpretation of the references to colour in this figure legend, the reader is referred to the web version of this article.)

2. Material and methods

2.1. Study site, sample collection

The MOBYDICK cruise took place during the late Austral summer (from 19 February to 20 March 2018), where samples were collected at four stations (M1, M2, M3, and M4. Fig. 1). Station M2, above the Kerguelen plateau, was located in naturally iron-fertilized waters (Blain et al., 2007), characterized by intense phytoplankton blooms during spring and summer (Mosseri et al., 2008; Cavagna et al., 2014). Stations M1, M3, and M4, situated off-plateau, were in an oceanic area of HNLC (High-nutrient, low-chlorophyll) waters (Cavagna et al., 2015). The sampling strategy included repeated visits at the different stations. Station M2 was sampled three-times at eight day intervals (M2–1, M2–2, and M2–3); stations M3 and M4 were sampled twice with two-week intervals (M3–1, M3–3, M4–1, and M4–2); and station M1 was sampled just once (Table 1). Samples were collected with 12 L Niskin bottles mounted on a rosette equipped with CTD (SeaBird 911-plus).

Pigments were analyzed using High Performance Liquid Chromatography (HPLC, Ras et al., 2008). CHEMTAX analysis was performed with CHEMTAX v1.95 (Mackey et al., 1996) to estimate the pigment:Chl *a* ratios for seven major phytoplanktonic groups: chlorophytes, prasinophytes, cyanobacteria, cryptophytes, diatoms, dinoflagellates, and haptophytes (detailed in Irion et al., 2020). Pigments and microzooplankton data (see below) from the onset of the bloom (early spring, October–November 2011, KEOPS2 cruise, Georges et al., 2014, Christaki et al., 2015) were included here for comparison with post-bloom MOBYDICK period (this study); KEOPS2 pigments were analyzed with CHEMTAX as described above.

2.2. Molecular analysis

Water samples were collected at all stations (M1, M2, M3, and M4) at four depths (15 m, 60 m, 125 m, and 300 m). The depths were chosen to correspond to the surface and the bottom of the mixed layer (ML), the transition between surface and deeper waters (125 m), and the deep nutrient rich waters (300 m). After pre-filtering though 100 μm mesh to remove most of the metazoans, 10 L of seawater from each depth were filtered successively through 20 μm and 0.2 μm using a peristaltic pump ('large' and 'small' size fractions, respectively). Filters were stored at −80 °C until DNA extraction. The extraction, PCR procedure, and downstream analysis are described in detail in Sassenhagen et al. (2020). Briefly, extraction was realized with PowerSoil DNA Isolation Kit (QIAGEN, Germany) following standard manufacturer's protocol. The 18S rDNA V4 region was amplified using EK-565F (5'-GCAGTTAAAAAGCTCGTAGT) and UNonMet (5'-TTTAAGTTTCAGCCTTGCG) primers (Bower et al., 2004). Libraries were paired-end (2 × 300 bp) Illumina MiSeq sequenced. The forward and reverse reads were demultiplexed using Qiime1 pipeline (Caporaso et al., 2010). The reads were further trimmed and filtered in the *R*-package DADA2 (Callahan et al., 2016). The same package was used for identification of amplicon sequencing variants (ASV) and their taxonomical assignment based on the PR^2 database (Guillou et al., 2012). ASVs affiliated to Metazoa, Streptophyta, as well as rare ones with less than 15 reads in the whole data set, were removed with the *R*-package 'phyloseq' (McMurdie and Holmes, 2013).

To investigate the phylogenetic relationship between the observed genera, the sequences generated in this study and additional sequences from the Genbank database were aligned using the software muscle 3.8.31 (Edgar, 2004) with default settings. The alignments were trimmed with the software trimAl v1.2 (Capella-Gutierrez et al., 2009) applying a gap threshold of 0.6. Maximum likelihood trees were separately build for DIN and CIL with the software RAxML version 8.2.12 (Stamatakis, 2014) using the substitution model "GTRCAT". The RAxML settings included rapid bootstrap analysis, while the number of distinct starting trees was based on bootstrapping criteria. The tree was

Table 1
Station description, coordinates and depth of the CTD 'stock'. The depth of the mixed layer (Z_{ML}) is based on a difference in sigma of 0.02 to the surface value. The mean Z_{ML} and Ze (Ze = 1% light depth) of all CTD casts performed during the occupation of the stations is given. For the rest of the variables the mean ± SD is given for the mixed layer. **EARLY SPRING**: Onset of the bloom, KEOPS2 cruise (KErguelen Ocean and Plateau compared Study project, 2011), **LATE SUMMER** post-bloom MOBYDICK cruise (2018) on the plateau and ocean area of Kerguelen. The mean ML depht (Z_{ML}) of all CTD casts performed during the occupation of the stations is given. For the rest of the variables the mean ± SD is given for the mixed layer except for GCP and NCP which is an integrated value in the ML. KEOPS2 station A3 was named M2 during the MOBYDICK cruise and has the same coordinates (cf Fig. 1). KEOPS 2, data from: Blain et al., 2015, Closset et al., 2014, Lasbleiz et al., 2016. MOBYDICK data of GCP and NCP from Christaki et al. 2021. NA: not available.

	EARLY SPRING					LATE SUMMER							
	On-plateau		Off-plateau			On-plateau			Off-plateau				
Station	A3–1	A3–2	R			M2–1	M2–2	M2–3	M1	M3–1	M3–3	M4–1	M4–2
Dates	20 Oct	16 Nov	26 Nov	26/10		6–8 Mar	16–17 Mar	8–9 Mar	3–5 Mar	18–20 Mar	28 Feb–3 Mar	12–14 Mar	6–8 Mar
Long-Lat (°E,°S)	72.1–50.6	72.1–50.6	66.7–50.4	50.3–66.7	66.7–50.4	72.0–50.4	72.0–50.4	72.0–50.4	74.5–49.5	68.0–50.4	68.0–50.4	67.1–52.3	67.1–52.3
Depth (m)	475	528	2450			520	519	527	2723	1000	1700	4186	4300
Z_{ML} (m)	105	168	105			62	61	68	27	65	79	49	87
Ze (m)	N/A	38	92		92	64	61	58	80	93	107	96	100
Chlorophyll a (μg L^{-1})	0.62 ± 0.17	2.03 ± 0.33	0.28 ± 0.04			0.27 ± 0.02	0.30 ± 0.04	0.58 ± 0.02	0.35 ± 0.040	0.20 ± 0.02	0.14 ± 0.00	0.18 ± 0.01	0.21 ± 0.00
$NO3^- + NO2^-$ (μM)	29.7 ± 0.5	26.2 ± 0.4	26.0 ± 0.2			21.9 ± 0.12	21.79 ± 0.38	21.9 ± 0.08	25.2 ± 0.56	23.75 ± 0.31	23.34 ± 0.12	25.7 ± 0.05	24.8 ± 0.27
PO_4^{3-} (μM)	2.00 ± 0.03	1.78 ± 0.03	1.83 ± 0.03			1.47 ± 0.03	1.50 ± 0.04	1.50 ± 0.00	1.71 ± 0.11	1.65 ± 0.05	1.08 ± 0.92	1.70 ± 0.02	1.71 ± 0.01
$Si(OH)_4$ (μM)	23.7 ± 0.8	18.9 ± 0.5	12.3 ± 0.3			1.36 ± 0.41	1.72 ± 0.79	2.75 ± 0.27	8.38 ± 2.93	2.89 ± 1.01	2.31 ± 0.04	4.36 ± 0.35	4.80 ± 0.00
GCP (mmol C m^{-2})	N/A	344	134			105	213	83	121	nd	132	187	129
NCP (mmol C m^{-2})	N/A	237	57			30	100	44	52	nd	15	88	106

visualized with the online application iTOL (Letunic and Bork, 2016).

2.3. Microscopic analysis

At each station, microzooplankton samples were taken from 10 to 12 depths between the surface and 300 m. Sample volume was 500 mL from surface to 200 m, and 1 L at 300 m. Samples were fixed with acid Lugol's solution (2% *v*/v). All samples were kept at 4 °C in the dark until microscopy analysis. In the laboratory, samples were left to settle in graduated cylinders for four days, then the 100 mL bottom of each sample was transferred into settling chambers and left to settle for another 24 h before examination under an inverted microscope (Nikon Eclipse TE2000-S; x400). DIN and CIL were identified based on their morphology at the lowest possible taxonomic level following (Tomas, 1997; McMinn and Scot, 2005; Kofoid and Campbell, 1929; Schiller, 1931–1937; Petz, 2005; Georges et al., 2014). DIN and CIL were also classified into six size classes (<20, 20–40, 40–60, 60–80, 80–100, and > 100 μm). Linear dimensions were measured at x400 magnification using an image analyzer with a camera mounted on the microscope. Biovolume measurements were converted into biomass using a conversion factor of 190 fg C μm^{-3} (Putt and Stoecker, 1989) and 0.760 x $volume^{0.819}$ pg C μm^{-3}, respectively (Menden-Deuer and Lessard, 2000).

2.4. Microzooplankton herbivory via dilution experiments

Dilution experiments were conducted at all stations following the protocol of Landry and Hassett (1982). However, due to a change in shipboard operational procedure at station M3–3, a significant increase in incubator water temperature occurred. Although samples were analyzed, (phytoplankton growth almost doubled while grazing remained of the same levels) the results are not presented here. Fifty liters of subsurface seawater, representative of the mixed layer, were collected at 30 m depth with Niskin bottles and gently screened through a 200 μm sieve to remove metazoans. Twenty liters of 0.2 μm filtered seawater (FSW) were prepared through low-pressure filtration (<50 mmHg). Five different concentrations (10%, 25%, 50%, 75%, and 100%) were prepared by mixing <200 μm and < 0.2 μm filtered seawater. For each treatment, three 2.4 L polycarbonate bottles were filled to the rim by gently siphoning from the carboys. Light measurements prior to incubation indicated that 25% light was available between 19 and 35 m (average: 25 ± 6 m) which matched with the sampling depth (30 m) for the dilution experiment. Thus, 25% light was the best compromise between experimental constraints and field measurements. All 15 bottles were incubated for 24 h in an on-deck incubator connected to the flow-through sea surface-water system and covered with a lid that let 25% of PAR light through (equivalent light condition to in situ surface waters). Additionally, 2.4 L were set aside for immediate sampling at T0. For Chl *a* measurement at the end of the incubation, 500–700 mL from each bottle were filtered onto 0.2 μm polycarbonate filters (ø 47 mm). After filtration, each filter was placed into 2 mL cryotubes, flash frozen in liquid nitrogen and stored at −80 °C. Chl *a* concentrations were estimated by fluorometry. Filters were extracted overnight in 90% acetone at 4 °C. At the end of the extraction period, Chl a concentration was determined using a calibrated Turner Trilogy© fluorometer. Initial Chl a concentration for each dilution treatment was estimated by multiplying initial whole seawater Chl a concentrations by corresponding dilution factors. Assuming a phytoplankton exponential growth, changes in Chl a concentration over the experiment were used to calculate the instantaneous phytoplankton growth (k, d^{-1}), and grazing mortality (g, d^{-1}, Landry and Hasset 1982, Fig. A1). Grazing pressure (% Chl a production d^{-1}) has been calculated as the ratio between phytoplankton daily production (μg Chl a L^{-1} d^{-1}) and microzooplankton daily consumption (μg Chl a L^{-1} d^{-1}).

2.5. Data analysis

Co-inertia analysis (PCA-PCA COIA) was used to investigate the coupling between phytoplankton pigments and CIL and DIN communities (Doledec and Chessel, 1994; Dray et al., 2003). The abundances obtained through microscopic counts of the 16 most abundant genera (8 DIN and 8 CIL), representing >90% of total abundance at each station were used. COIA differs from other 'classic' canonical models in utilizing partial least-squares regression, rather than multiple regression, to summarize common structure. Because COIA is based on partial least-squares regression, it places no restrictions on the number of variables that can be analyzed (unlike the classic canonical models). The co-inertia model is symmetric, and therefore descriptive rather than predictive (for more details Kenkel, 2006). COIA defines axes that simultaneously explain the highest possible variance in each of the two matrices and describes their closest possible common structure. In a 'PCA-PCA COIA' as applied here, a PCA (principal component analysis) was performed on each matrix prior to applying a COIA analysis.

A PCA (principal component analysis) was performed on each matrix prior to applying a COIA analysis (Dray et al., 2003). For PCA analysis, variables were standardized and PCA was performed using the R-package FactoMineR (Lê et al., 2008). COIA was carried out with the 'ade4' package in *R*-software (Dray and Dufour, 2007). The strength of the coupling between the two matrices, in COIA is expressed by the multidimensional correlation coefficient (RV), and statistical significance was tested using a Monte Carlo permutation procedure with 1000 permutations. Finally, in order to define the variables that were the most important in structuring the COIA scatterplot, Pearson's correlation coefficients were calculated between all variables and COIA coordinates. All statistical analyses were based on abundances from microscopical counts to avoid the biases of the sequencing data (see results and discussion sections).

3. Results

3.1. Environmental conditions and phytoplankton composition

The four stations sampled during MOBYDICK were situated in different hydrological conditions. Station M1, which was situated in Antarctic waters and influenced by the polar front, was characterized by a shallow Z_{ML} (27 m, Table 1, Figs. 1 and 2). Stations M2 and M4, which were situated south of the polar front in Antarctic waters, presented a characteristic temperature minimum at 200 m and showed the lowest surface temperature (at M4: 4.5 °C) (Table 1, Figs. 1 and 2). Station M3, which was situated in sub-Antarctic waters (SAZ), showed the highest temperature in the ML (5.6 °C, Table 1). The Z_{ML} deepened at all stations following a storm on the 10th of March 2018. Phosphate and nitrate concentrations were high at all stations while silicic acid was overall higher off-plateau (Table 1). For comparison with early spring (KEOPS2 cruise), stations A3 (on-plateau) and R (defined as the reference station off-plateau) are also shown in Fig. 1 and Table 1. Briefly, A3–1 was sampled in late October, just before the initiation of the bloom. A3–2 was explored about 3.5 weeks later, during the onset of the bloom. During early spring, the Z_{ML} at these stations was >100 m (Table 1, Christaki et al., 2014) . During MOBYDICK, Chl a in the Z_{ML} doubled between the first and the third visit at M2 (from 0.27 to 0.58 μg L^{-1}). Chl a at the off-plateau stations ranged between 0.14 and 0.35 (M3–3 and M1, respectively (Table 1, Fig. 1). The concentrations of group pigment signatures analyzed with CHEMTAX illustrated the phytoplankton community structure. Diatoms and prymnesiophytes were always the two major groups. Their respective proportions varied between seasons (early spring or late summer) and positions (on- or off-plateau). Diatoms were dominating during early spring (74–94% of total Chl a in on-plateau water; Fig. 3a, b) while prymnesiophytes were the most abundant phytoplankton group during late summer (37–53% and 59–70% of total Chl a in on- and off-plateau, respectively; Fig. 3a, b). The third

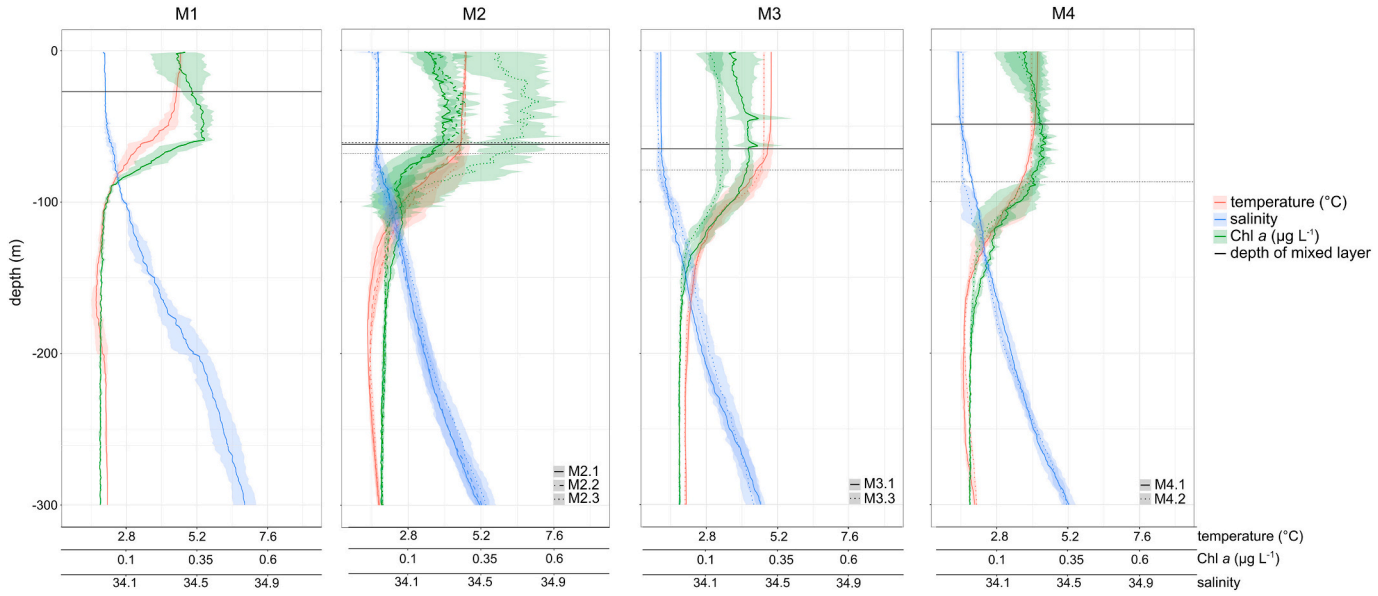

Fig. 2. Mean profiles of Temperature (°C), Salinity and Chl-*a* (derived from in vivo fluorescence) calculated from all the CTDs of each visit to a station. Shadows are standard deviations around the mean of all CTDs sampled at each station.

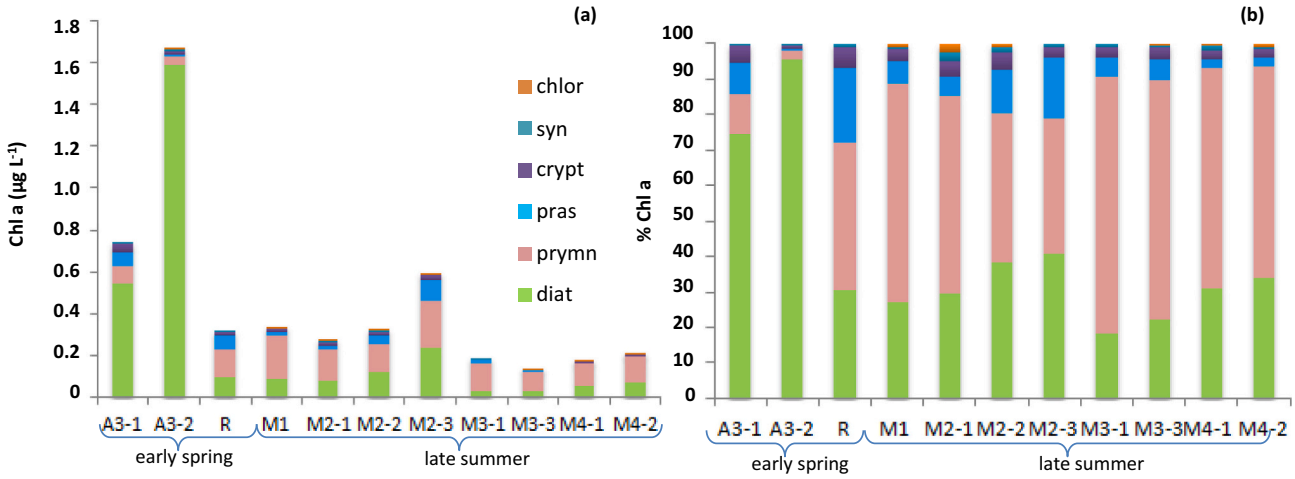

Fig. 3. Mean contribution and relative contribution of pigments to total Chl. diat = diatoms, prymn = prymnesiophytes, pras = prasinophytes, crypt = cryptophytes, syn = *Synechoccocus*, chlor = chlorophytes. A3–1, A3–2 and R: correspond to early spring data (KEOPS2, cruise). Late summer: MOBYDICK cruise.

group contributing most to the phytoplankton biomass were picoplanktonic prasinophytes that accounted for up to 21% of Chl a during early spring in HNLC waters (R-2) and up-to 16.5% of Chl a on the plateau during late summer (M2–3).

3.2. Microzooplankton communities

3.2.1. Abundance, biomass distributions and morphological diversity

During MOBYDICK, microscopy observations allowed the identification, size measurement, and biomass estimation of dinoflagellates (DIN) and ciliates (CIL) (Fig. 4 a–f). Mean integrated abundance in the mixed layer showed that DIN were from 3 to 6 fold more abundant than CIL in the ML and varied between 0.29 and 2.3 $\times$ 10^3 and 0.28 to 0.45 $\times$ 10^3 cells L^{-1} for DIN and CIL, respectively (Fig. 4 a, c). During late summer, DIN were largely dominated by the <20 µm size fraction (63–85% Fig. 4b) while CIL were mostly represented by the 20–40 µm and < 20 µm size fractions (mean 50 and 32%, respectively, Fig. 4d). The biomass of DIN was higher than CIL by factors of 1.3–2.3 at five out of the eight stations. DIN and CIL had, however, equal biomass at M2–2, M1, and M3–3 (Fig. 4 e, f). The DIN + CIL biomass was slightly higher at M2 (mean 3.5 $\pm$ 0.2 µg L^{-1}) than off-plateau (2.2 $\pm$ 0.3 µg L^{-1}, Fig. 4e). The vertical profiles did not show any noticeable evolution over time at M2 or at the other stations (Fig. 5).

A total of 40 morphotypes of DIN and CIL were identified by microscopy at the highest possible taxonomic level. The 23 identified DIN-morphotypes belonged to 13 genera. The genus *Gymnodinium* (<20 µm in size) was the most abundant DIN and largely prevailed at all stations (Fig. 6a). Other small sized DIN such as *Scripsiella, Prorocentrum compressum*, and *Amphidinium* were present and abundant at all stations. The larger size classes were represented by *Tripos* and *Dinophysis*, while a variety of *Protoperidinium* morphotypes belonged to small and larger size classes. As for abundance and biomass, DIN richness and community structure were similar at all stations on- and off-plateau (Fig. 6a). The 13 CIL-morphotypes covered 11 genera. *Lohmaniella oviformis* (<20 µm in size) was the most abundant CIL at all stations, with the exception of M3 where the tintinnid *Cymatocylis antarctica* prevailed (Fig. 6b, Table 2). *Leegardiella*, *Codonelopsis soyai*, *Salpingella acuminata*, and *Myrionecta* were present at all stations at low abundances. Finally, the large

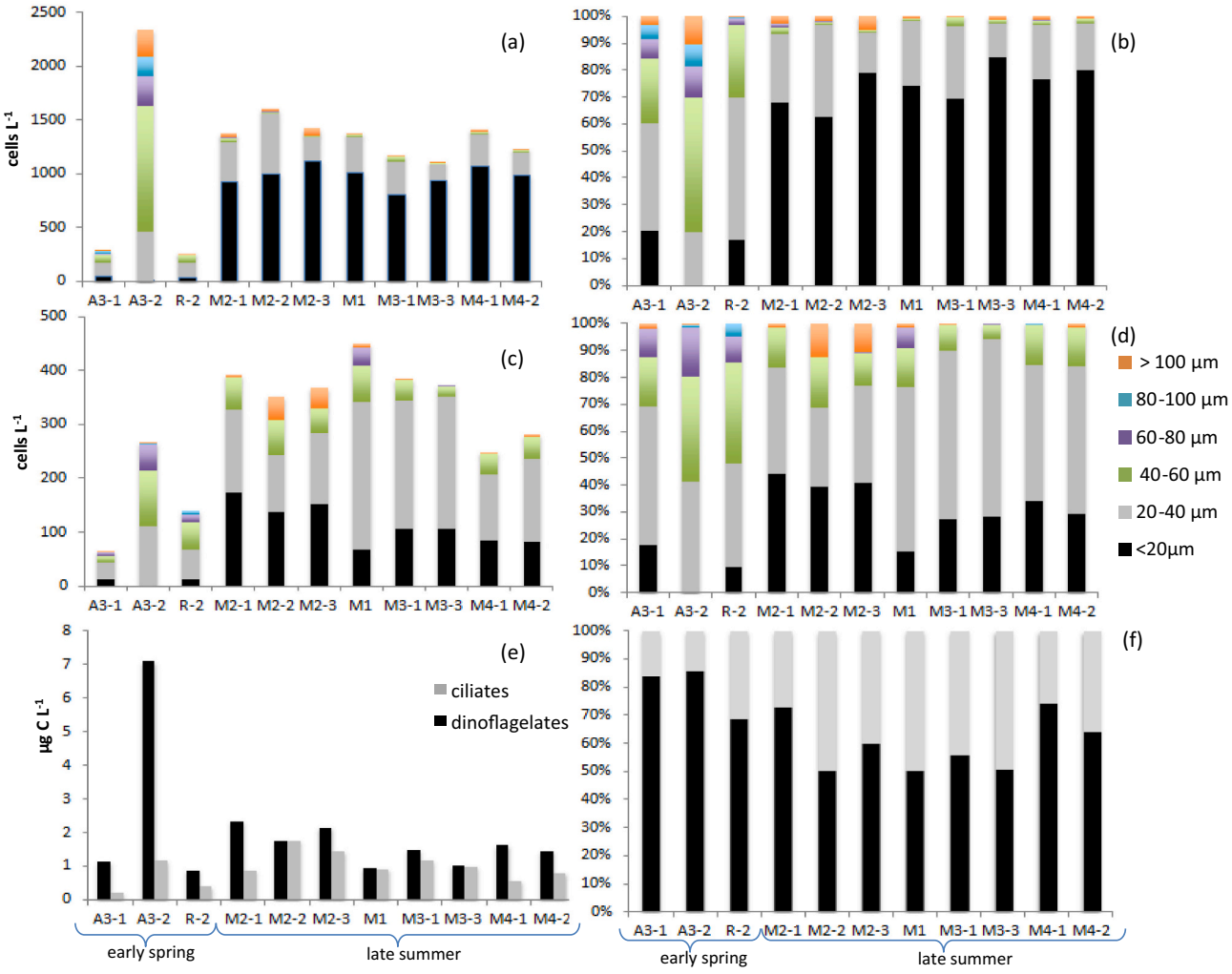

Fig. 4. Mean integrated abundances and relative abundance of dinoflagellate (DIN) size classes (a, b). Mean integrated abundances and relative abundance of ciliates (CIL) size classes (c, d) Mean integrated biomasses of DIN and CIL (e) and relative biomasses of DIN and CIL (f), in the mixed layer (ML).

mixotrophic *Laboea* was relatively abundant during the last two visits at M2, while it was rare at the other stations (Fig. 6b).

3.2.2. *Molecular diversity vs morphological diversity*

Heatmaps illustrating sequencing richness and relative abundance of DIN and CIL are presented in Fig. 6c, d. After downstream analysis and elimination of a few symbionts and parasites (e.g., *Blastodinium* and *Chytriodinium*), the class Dinophyceae was represented by 31 ASVs. (Fig. c). ASVs affiliated to *Tripos* were the most abundant ASVs among those affiliated to DIN (% of reads) in the large size fraction. In the small size fraction, *Tripos* and *Gymnodinium* ASVs were more or less equally represented (Fig. 6c). As in microscopy data, *Gyrodinium* and *Prorocentrum* were also among the most abundant in terms of proportions of reads. However, *Scrippsiella* and *Amphidinium*, which were abundant in microscopy, were not found in sequencing data (Fig. 6a, c). A maximum likelihood tree (Fig. 7a) was constructed in order to visualize the relatedness of taxa identified by microscopy and sequencing. Besides sequences generated in this study, additional sequences from the Genbank database corresponding to missing genera observed only by microscopy (e.g., *Amphidinium* and *Scrippsiella*) were included. The DIN genera *Oxytoxum* and *Katodinium,* which were observed by microscopy, were not represented by sequences in the Genbank or in the PR^2 (Guillou et al., 2012) databases. They were therefore not included in the tree (Fig. 7a). Most DIN genera in the maximum likelihood tree did not cluster by order, which was especially evident for Gymnodiniales and Peridiniales (Fig. 7a). The abundance ranking of taxa differed between sequencing and microscopy (Fig. 6a,c).

The ciliate ASVs were grouped into 40 approximate genera with often uncertain taxonomic affiliations below the class or order level (Fig. d). The maximum likelihood tree for CIL included sequences from this study and additional sequences from the Genbank database corresponding to missing genera observed only by microscopy (*Myrionecta, Scuticociliatia,* and *Laboea*). The CIL maximum likelihood tree was better resolved than the tree for the DIN with almost all genera clustering by order. The CIL *Codonelopsis* and *Lohmaniella, L. oviformis* were the most abundant taxa based on microscopy, but were lacking from the tree since they were not represented by sequences in public databases (Fig. 7b). At M3–1 and M3–3, an ASV affiliated to the tintinnid family Xystonellidae prevailed in the large size fraction (20–100 µm) while *Cymatocylis calyciformis* was the most abundant tintinnid in the microscopy dataset (Fig. 6 c, d). *Myrionecta* is a cosmopolitan CIL characterized by a particular morphology and also several morphotypes grouped into "scuticociliates" were observed by microscopy but were not retrieved by sequencing.

3.3. *Microzooplankton relation with pigment signatures*

COIA analysis was applied to test for spatiotemporal relation in DIN + CIL community composition and phytoplankton pigments (Fig. 8a-e). Hierarchical clustering and PCA of DIN + CIL abundances applied as the

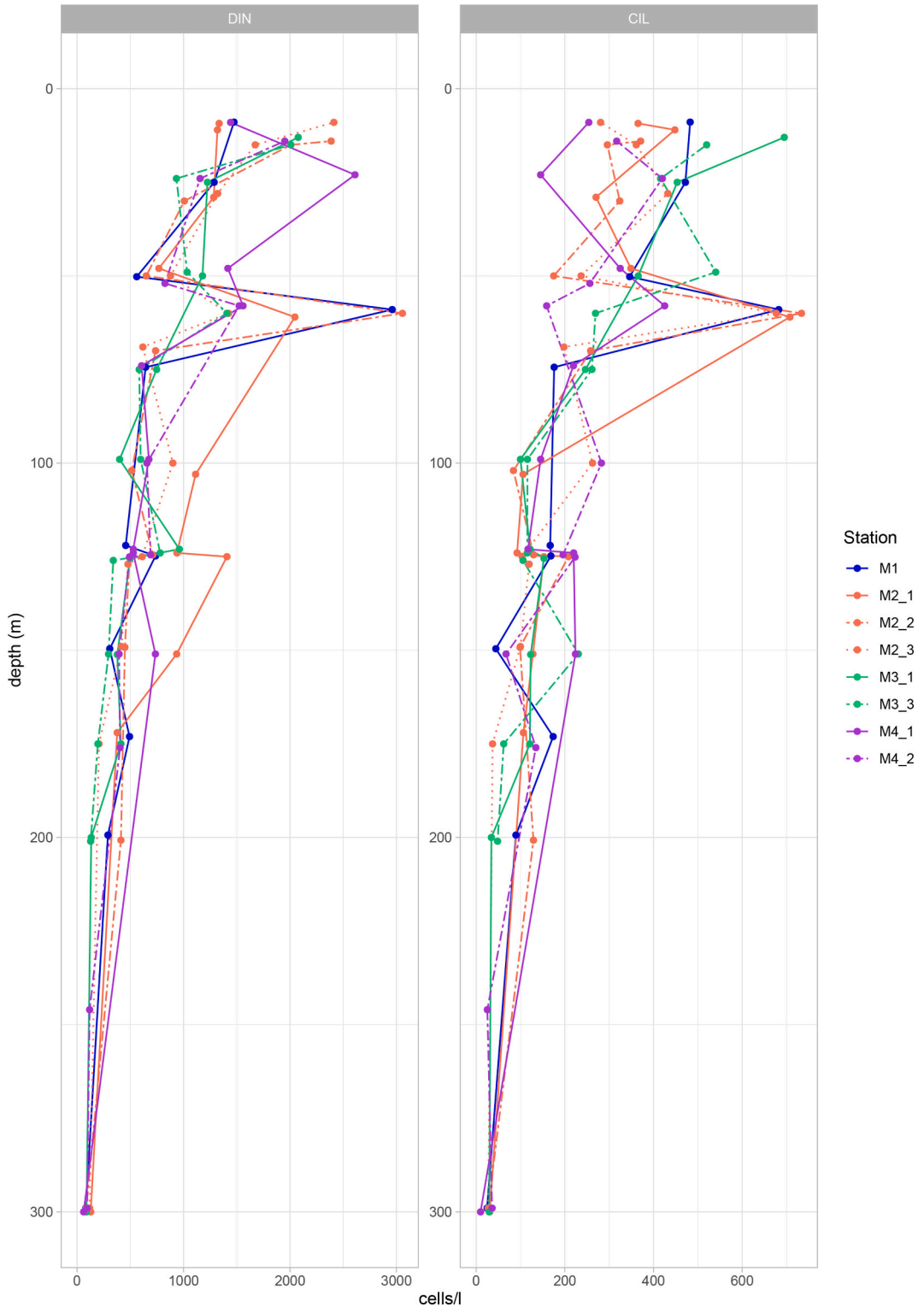

Fig. 5. Vertical profiles of dinoflagellates (DIN) and ciliates (CIL) during the MOBYDICK cruise.

first step of the COIA analysis revealed that the on- and off- plateau MOBYDICK stations grouped together (Fig. 8a, c). A3–1, sampled in early spring before the onset of the bloom, grouped with the reference HNLC station (R, sampled during the same cruise), while A3–2 was highly differentiated from all stations in the PCA (Fig. 8a, c). In fact, PCA suggested that station A3–2 was characterized by the presence of the diatom consumers *Gyrodinium* and *Protoperidinium.* In contrast, all MOBYDICK stations were featuring *Gymnodinium*, *Leegardiella*, *Lohmaniella*, *Scripsiella* and Tintinninds (Fig. 8c). Hierarchical clustering and PCA performed on pigment data indicated similar phytoplankton communities at off-plateau stations during the MOBYDICK cruise. The PCA highlighted a gradual change in pigment signature during the three visits at M2 related to an increase in prasinophyte pigment concentrations. The station A3 was uniquely characterized by high concentrations of diatom pigments and Chl *a* (Fig. 8b, d see also Fig. 3). The COIA multidimensional correlation coefficient (RV) used to estimate the

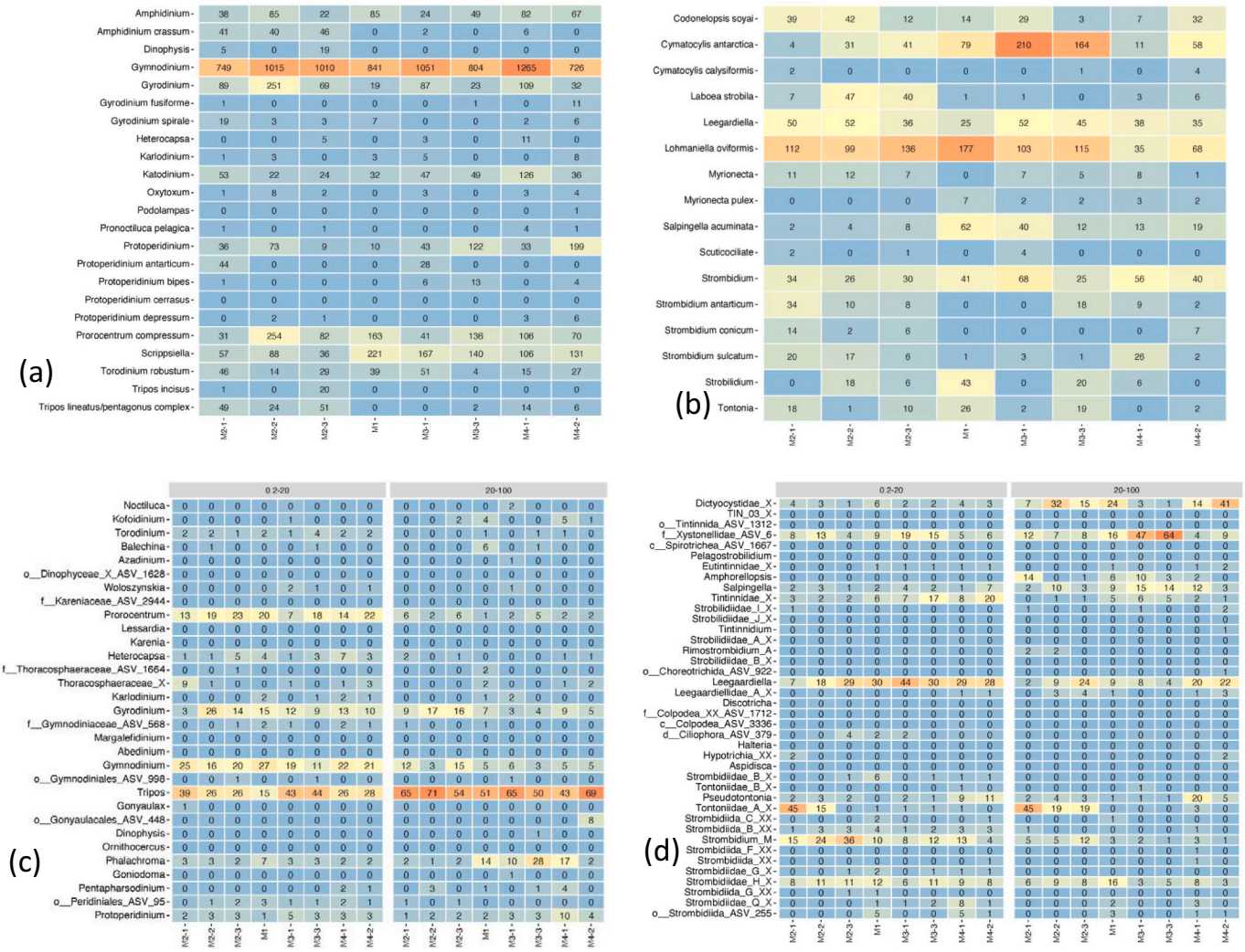

Fig. 6. Heatmaps illustrating microscopy (a, b) versus sequencing (c, d) diversity and abundance data for dinoflagellates (DIN) ciliates (CIL) during MOBYDICK. DIN and CIL microscopy data values are the mean integrated abundances of cells in the ML (cells L^{-1}) (a and b, respectively). DIN and CIL sequence data illustrate relative abundance of reads in the 0.2–20 and 20–100 μm size fractions in the class Dinophyceae (c) and, the relative abundance of reads in the 0.2–20 and 20–100 μm size fractions in the division Ciliophora (d).

Table 2
Dilution experiment derived phytoplankton growth and microzooplankton grazing parameters.

	On-plateau			Off-plateau			
Station	M2–1	M2–2	M2–3	M1	M3–1	M4–1	M4–2
Initial Chl a (10-20 m depth, μg L^{-1})	0.30	0.36	0.64	0.35	0.20	0.20	0.26
Phytoplankton growth rate (d^{-1})	0.13 ± 0.03	0.15 ± 0.02	0.26 ± 0.03	0.22 ± 0.02	0.17 ± 0.12	0.08 ± 0.03	0.18 ± 0.09
Microzooplankton grazing rate (d^{-1})	0.34 ± 0.05	0.37 ± 0.04	0.53 ± 0.05	0.28 ± 0.03	0.50 ± 0.20	0.38 ± 0.05	0.43 ± 0.15
Dilution determination coefficient (r^2)	0.86***,**	0.90***	0.81***	0.89***	0.35*	0.83***	0.45*
Phytoplankton daily production (μg Chl a L^{-1} d^{-1})	0.04 ± 0.009	0.05 ± 0.008	0.17 ± 0.02	0.08 ± 0.006	0.03 ± 0.02	0.02 ± 0.006	0.05 ± 0.02
Microzooplankton daily consumption (μg Chl a L^{-1} d^{-1})	0.08 ± 0.01	0.13 ± 0.01	0.33 ± 0.03	0.10 ± 0.01	0.10 ± 0.04	0.07 ± 0.008	0.10 ± 0.04
Grazing pressure (%Chl a production d^{-1})	213.10	231.68	194.06	130.05	287.48	427.88	219.86

*** $p < 0.001$.
** $p < 0.01$.
* $p < 0.05$.

strength of coupling between the pigment concentration and microzooplankton abundance was significant (RV = 0.602, $p = 0.005$) and the first two axes explained 85.65% of the projected variance (Fig. 8e). All the pigments showed significant correlations ($p < 0.05$, Table A1) with at least one of the three first axes, while ten out of the sixteen genera used for the analysis showed significant correlations: *Gymnodinium*, *Gyrodinium*, *Scripsiella*, *Amphidinium*, *Tripos*, *Lohmaniella*, *Strombidium*, *Leegaardiella*, *Salpingella*, and *Myrionecta* (Table A1). The COIA scatterplot indicated the station position relative to their DIN, CIL and pigment variables. On the COIA scatterplot MOBYDICK off-plateau stations formed one group with M1 being slightly differentiated potentially due to the influence from the Polar Front. The position of station M1 also changed most between the two PCA-Biplots, as its microzooplankton community strongly resembled the communities at the other off-plateau

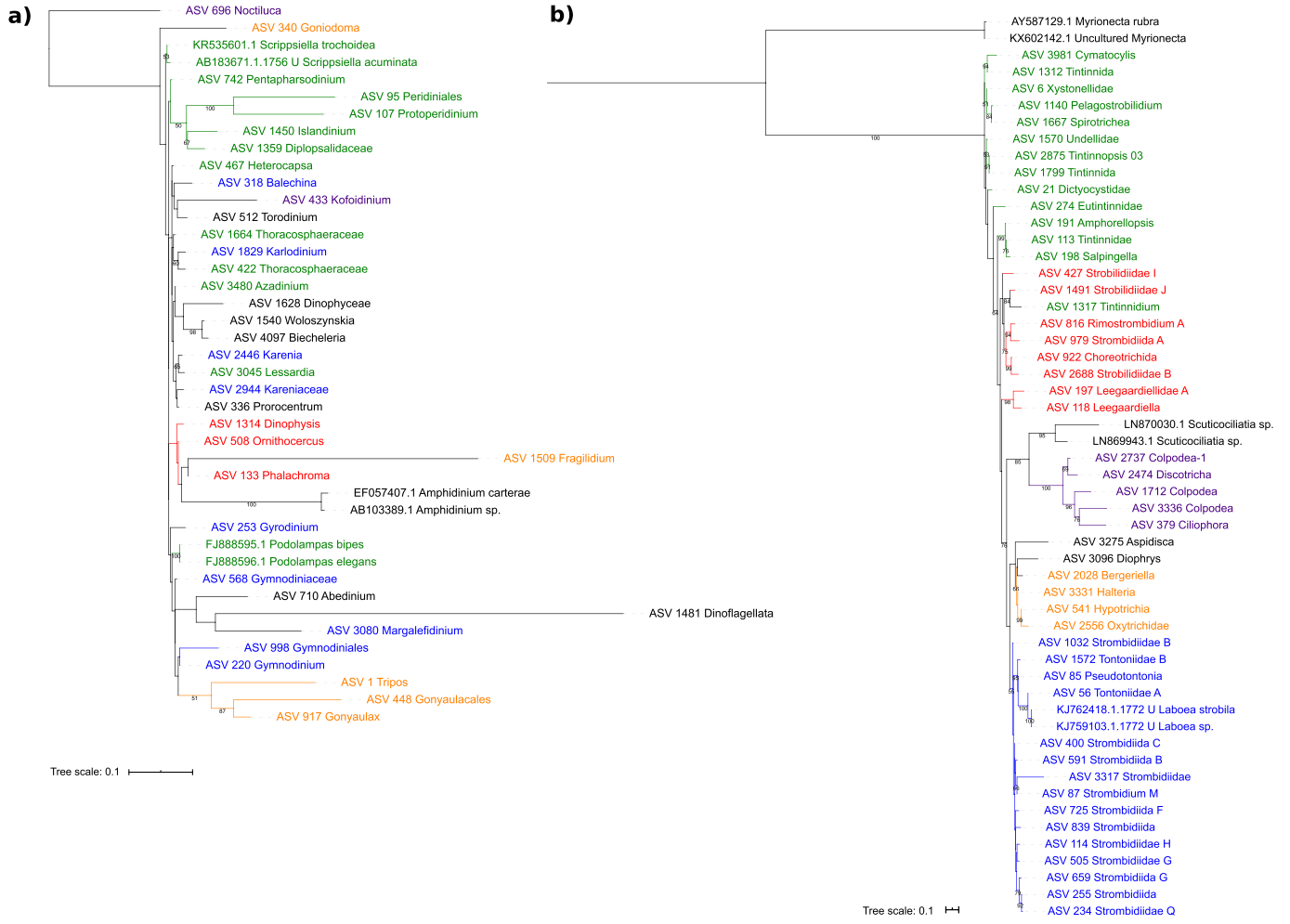

Fig. 7. Maximum likelihood trees for dinoflagellate (DIN)(a) and ciliate (CIL)(b) genera. Bootstrap values >50 are indicated on branches. Tree scales refer to the length of branches and indicate the mean number of substitutions per site. Genera are coloured by order. a) DIN topology. Purple = Noctilucales, blue = Gymnodiniales, green = Peridiniales, orange = Gonyaulacales, red = Dinophysiales, black = individual orders for each genus. b) CIL topology. Green = Tintinnida, red = Choreotrichia, purple = Colpodea, orange = Hypotrichia, blue = Strombidiida, black = Cyclotrichiida (Myrionecta), Scuticociliatia, Euplotia (Diophrys, Aspidisca). (For interpretation of the references to colour in this figure legend, the reader is referred to the web version of this article.)

stations, while its pigment signature was more similar to station M2–2. The first two visits at M2 were close together, while M2–3 was closer to the early spring reference station R, with which it shared a stronger prasinophyte signature. Station A3–2, uniquely representing typical bloom conditions with high diatom pigments and microphytoplankton grazers, was far apart from the other stations in this plot (Fig. 8e).

3.4. *Microzooplankton herbivory via dilution experiments*

In situ (10-20 m depth) Chl *a* concentration measured at the beginning of the dilution experiment varied from 0.20 to 0.64 μg Chl *a* L^{-1} (M3–1 and M2–3, respectively). Dilution derived phytoplankton growth (k) and microzooplankton grazing (g) were significant at all stations (Table 2, Fig. A1). Phytoplankton growth rate (k) ranged from 0.08 ± 0.03 d^{-1} at M4–1 to 0.26 ± 0.03 d^{-1} at M2–3. Minimum microzooplankton grazing rates (g) were measured at station M1 (0.28 ± 0.03 d^{-1}) and the maximum value was at station M2–3 (0.52 ± 0.05 d^{-1}). Phytoplankton mortality due to microzooplankton grazing was always higher than phytoplankton growth, representeing 130 to 428% of phytoplankton daily production at M1 and M4–1, respectively. Overall, phytoplankton growth rate increased at station M2 (0.13 ± 0.03 to 0.26 ± 0.03 d^{-1}) along with microzooplankton grazing (0.34 ± 0.05 to 0.52 ± 0.05 d^{-1}, Table 2).

4. Discussion

The present study showed that ciliates were always recorded at considerably lower abundances than dinoflagellates. The diversity assessed by Illumina sequencing of 18S rDNA amplicons and microscopic observations could be compared with microscopy at a relatively high taxonomic level (i.e., often to family level). In particular for dinoflagellates, relative abundances and ranking of dominant taxa differed between sequencing and microscopy observations. Dilution experiments suggested significant grazing of microzooplankton on phytoplankton as phytoplankton net growth (k) was lower than microzooplankton grazing (g) at all stations. Despite its great potential as phytoplankton grazer, microzooplankton occurred at low biomass and showed little temporal variability, suggesting that it was controlled by copepod predation. These important results are discussed below.

4.1. *Microzooplankton diversity - microscopy vs sequencing*

Massive sequencing technologies such as Illumina MiSeq gain *in momentum* (e.g., Pawlowski et al., 2012) and are currently used to describe global patterns of plankton and even predict carbon export (e.g., Guidi et al., 2016, Obiol et al., 2020, among many others). The recent ASV approach is supposed to provide a more accurate image of the

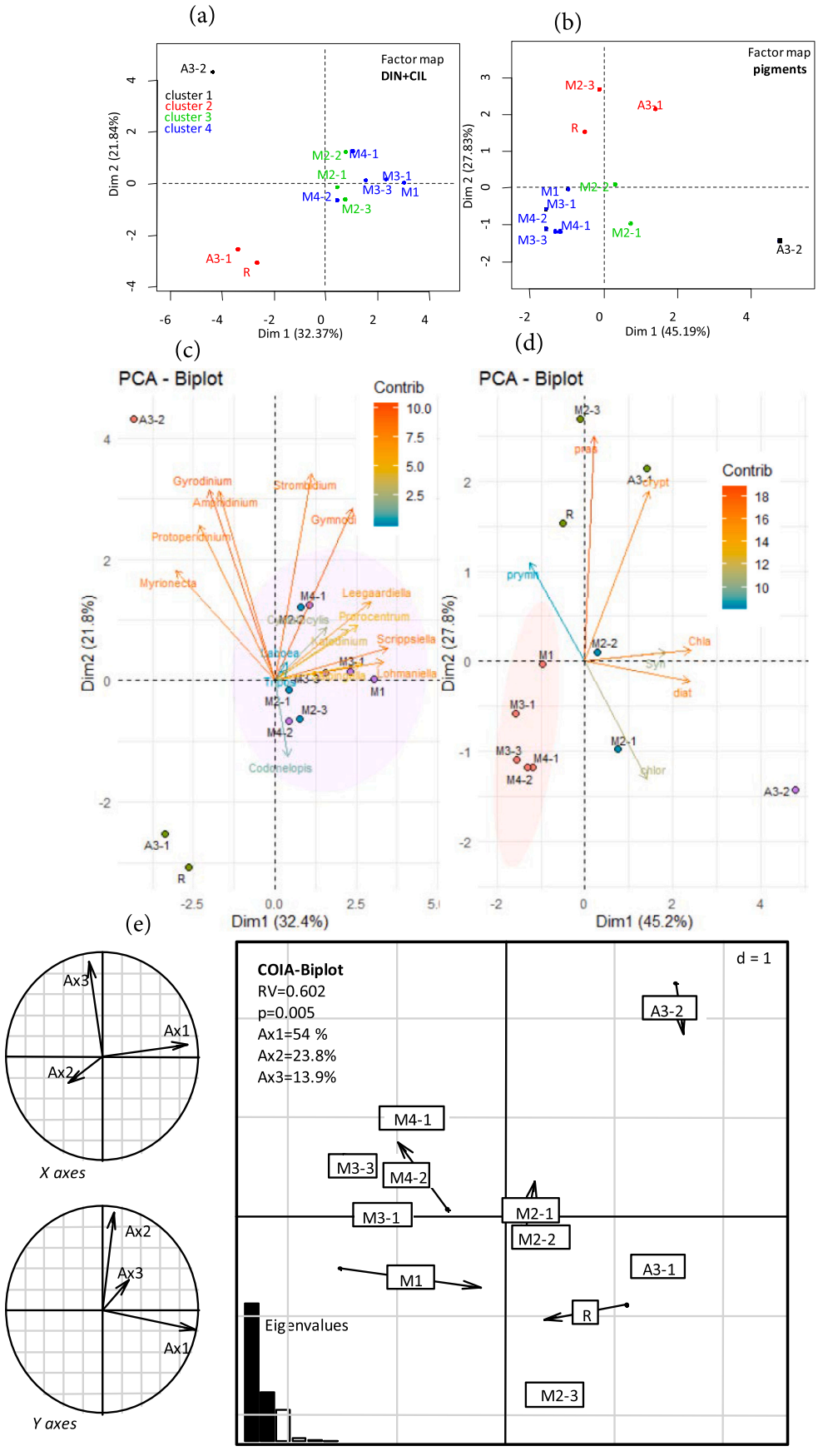

Fig. 8. Co-inertia analysis (PCA – PCA COIA) between the 16 most abundant DIN + CIL genera and characteristic pigments. The two Hierarchical Clustering Factor Maps and the two PCA applied to each table are the intermediate steps of the analysis before the final COIA-Biplot. They are presented here in order to better follow the text of Section 3.3. Hierarchical Clustering Factor Maps indicate station groupings according to the DIN and CIL dominant genera (a) and pigments concentrations (b). Also presented are the results of the Principal Component Analysis (PCA) of DIN + CIL (c) and pigments (d) with their contribution to the first two principal components, and finally the synthesized COIA results (e). The *x*-axes show projections of the first 3 PCA components from the pigments while the *y*-axes show those of the genera (e). The circles represent a view of the rotation needed to associate the 2 datasets. *P*-values were calculated using Monte Carlo permutation tests (1000 permutations). The sample scatterplot shows how far apart the samples were relative to their pigment and taxonomic variables (e). The beginning of the arrow shows the position of the sample described by the pigments, and the end by the microzooplankton genera. RV: correlation coefficient between the 2 tables ('R' for correlation and 'V' for vectorial) (e).

diversity by avoiding artificial similarity thresholds. Nevertheless, organisms differing by a few base pairs in their rDNA can belong to very different taxa and the threshold of differences in the rDNA sequence between species differs greatly from one taxonomic group to another one because of their evolution rate for example. Defining accurate taxonomy level based on the sequencing of rDNA remains a critical issue in microbial diversity investigations. In-depth sequencing and microscopy approaches are rarely confronted although they both 'miss' or 'misidentify' taxa due to the diverse biases inherent to each method (e.g., Medinger et al., 2010; Bachy et al., 2013; Charvet et al., 2012; Stern et al., 2018 and references therein). We address this by combining high throughput sequencing with microscopic observations to assess DIN and CIL diversity. Although microscopy and sequencing heatmaps (Fig. 6a-d) cannot be directly compared (different size fractions and water volumes analyzed for the two approaches), the diversity and abundance data obtained by the two approaches can be assessed to determine whether these results are conflicting or complementary. DIN were represented by 23 morphospecies in microscopy and 31 ASVs in sequencing data. Microscopic identification of dinoflagellates based on broad morphological features is challenging. On the other hand, amplicon sequencing does not provide accurate taxonomic resolution because of the lack of cultured representatives to provide a detailed phylogeny. This is the case for dinoflagellate taxa that are under-represented in databases, resulting in approximate taxonomic identifications of sequences and diversity estimates (e.g., Bik et al., 2012). Most DIN genera did not cluster by order in the topologic tree, which was especially evident for Gymnodiniales and Peridiniales (Fig. 7a). This insufficient resolution of DIN phylogeny might be due to the limited length and low variability of the V3-V4 region in the 18S rDNA (Daugbjerg et al., 2000; Mordret et al., 2018). A relatively good 'correspondence' was found between the two data sets in terms of diversity, but often at a higher taxonomic level, either at the family or order level (Fig. 6a, c). For example, the second most abundant genus found in microscopy identified as *Scrippsiella* was probably represented by the family level Thoracosphaeracea in sequencing data (Fig. 6a, c). However, no potential 'relative' for *Amphidinium* could be found in sequencing data (Fig. 7a). Sequencing complemented microscopy data in terms of diversity. Because the sample volume analyzed for microscopy counts is relatively limited, in contrast to the sequencing approach, low abundant taxa may not be observed by microscopy despite their characteristic morphological features. This was likely the case for the genus *Ornithocercus* (ASV 508) that was also retrieved in the vertically integrated plankton-net samples, where very large volumes of water were sampled (Karine Leblanc, https://plankton.mio.osupytheas.fr/mobydick-other-microplankton/). In addition, taxa relative abundance differed among sequencing and microscopy. It is well established that DIN are over-represented in sequencing data (e.g., Georges et al., 2014 and references therein). The dominance of *Tripos* in sequencing data - even in the small fraction - (Fig. 6c) highlighted that, even within the DIN population, specific taxa can be over-represented. As a consequence, using relative abundances of DIN based on sequence data in numerical analysis and/or description of community structure might lead to biases.

CIL were represented by 17 morphospecies in microscopy and 40 genera in sequencing data. The difficulty to accurately identify CIL based on broad morphology is exacerbated by the distortion of soft CIL due to chemical fixation. Only tintinnids having a lorica, preserve most of their features (e.g., Dolan et al., 2012). As for DIN, comparison of sequencing and microscopy data was challenging, in particular at the genus level, but could be attempted at higher taxonomic levels. Although, the CIL maximum likelihood tree had a better resolution than the topology of DIN, CIL sequencing and microscopy data could only be globally compared at a higher level than the DIN data (i.e., family, order, or class level). For example, *Lohmanniella oviformis*, which was the most abundant species in microscopy, was probably represented by *Leegardiella* in sequencing data (family Leegaardiellidae, Lynn and Montagnes, 1988). *Strombidium* was the second most abundant genus in both data sets. At M3–1 and M3–3, the family Xystonellidae, order Tintinnida prevailed in the large size fraction (20–100 μm) according to sequencing data. At the same stations, the dominant tintinnid in microscopy data was identified as *Cymatocylis calyciformis* that belongs to a different family (Ptychocylididae) but to the same order (Tintinnida) (Fig. 6 b, d). The organisms grouped into 'scuticociliates' in microscopy data probably belonged to different families or classes. Within the CIL populations, there was no evidence of over-representation of specific taxa and the ranking of the different taxonomic groups obtained by sequencing corresponded more or less to the one by microscopy. The taxonomic resolution obtained by sequencing was lower than the one obtained by microscopy (Fig. 6b, d).

As a conclusion, applying both sequencing and microscopy analyses to DIN and CIL can complement and enrich our view on the population diversity. However, if available, microscopy based abundances seem more reliable for numeric analysis. Using DIN relative abundances (retrieved from sequencing data) for numerical analysis could lead to misinterpretations of the importance of different taxa for ecosystem functioning. Therefore, morphological metadata can and should be collected in parallel to sequencing of DIN and CIL.

4.2. The relation of late summer microzooplankton communities to phytoplankton

Microzooplankton community structure and the biomass quantity are expected to relate to shifts in phytoplankton community composition (e.g., Grattepanche et al., 2011a; Lawerence and Menden-Deuer, 2012). Although other components of the microbial food web showed >2–3 fold higher abundance and activity on the plateau, and remained highly dynamic during the MOBYDICK cruise (Christaki et al., 2021; e.g., 2-fold increase in Chl *a* concentrations to 0.58 μg L^{-1} during the third visit to M2, Table 1), the DIN and CIL biomass was only ~1.5 x higher on-plateau (M2) compared to off-plateau and showed little temporal variability (e.g., Fig. 4). As a result, stations clustered differently based on pigment or microzooplankton data (Fig. 8a-d). The variability of the abundance of prasinophytes at M2, A3–1, R and the diatom increase at A3–2, were highlighted by the same analysis (Figs. 8c, d). The rapid increase in prasinophytes and diatoms on the plateau (M2 during MOBYDICK) was likely driven by changes in environmental conditions, such as NH_4 concentrations (Irion et al., 2020; Sassenhagen et al., 2020), which the microzooplankton community did not follow in the observed time frame. However, considering all data, the COIA analysis showed that there was an overall significant relationship between microzooplankton abundances and pigment concentrations ($p = 0.005$, Fig. 8e).

The maximum abundance of dinoflagellates and ciliates was often observed at the base of the ML (Table 1, Fig. 5, Christaki et al., 2008, 2015) and coincided with the formation of the deep chlorophyll maximum (DCM) (Lasbleiz et al., 2014). The formation of a DCM is described as a recurrent feature in the Southern Ocean, and is explained by the accumulation of inactive, though living, algal cells, mainly composed of diatoms (Uitz et al., 2009 and references therein).

The correlation between DIN biomass and phytoplankton abundance was especially noticeable during the onset of the diatom bloom on the plateau (Lasbleiz et al., 2016, Figs. 3 and 8, KEOPS2). The abundance and biomass of DIN increased 8 and 7 fold, respectively, within 3.5 weeks between the visits at station A3. In particular, large dinoflagellates such as *Gyrodinium* (40–60 μm), *Amphidinium* (20-40 μm) and *Protoperidinium*, which feed on diatoms and can ingest prey cells of more than 10 x their own size (e.g., Saito et al., 2006; Grattepanche et al., 2011b), occurred in higher abundance after the intensification of the bloom (Figs. 6a, 8, Christaki et al., 2015).

During MOBYDICK, a common feature of DIN and CIL communities was the relative importance of small cells (<40 μm) which was particularly pronounced for DIN (Fig. 4b). Small sized *Gymnodinium* were the most abundant DIN taxa at all stations and during both seasons (<20 μm,

Table 3
Summary of seasonal characteristics above the plateau of Kerguelen and in HNLC waters calculated for the mixed layer (ML). GCP and NCP: Gross and Net community production (cf. Table 1), phytoplankton, dinoflagellates (DIN), ciliates (CIL) dominant genera.

	Productivity regime (GCP)	Community respiration	DIN + CIL biomass	Phytoplankton	DIN	CIL	DIN + CIL carbon demand[a] as a % of GCP and NCP
	mmol C m^{-2} d^{-1}	% of GCP	mmol C m^{-2}				
Kerguelen Bloom							
Early spring	High[1] (344)	Low[1] 30%	High (116)	*Chaetoceros* *Thalassiosira* *some Phaeocystis* colonies [3,4]	*Gymnodinium, Protoperidinium* *Gyrodinium*[4,6]	*Strombidium* *Acanthostomella norvegica* *Codonellopsis soyai*[4,6]	18% GCP 25% NCP *(A3–2)*
Late summer	Moderate (134) [2]	Moderate[2] 57%	Low (15.4)	*Corethron*, *Phaeocystis* free cells *Micromonas* [5]	*Gymnodinium* *Gyrodinium* *Prorocentrum*	*Lohmaniella oviformis, Strombidium*	5.3 ± 2.4% GCP 14 ± 9.8% NCP *(mean ± sd of the 3 visits at M2)*
HNLC							
Early spring	Moderate (59) [1]	Moderate[1] 57%	Low (17)	*Phaeocystis Fragilariopsis*[3,4]	*Gymnodinium* *Gyrodinium* *Scripsiella*[4,6]	*Strombidium* *Codonellopsis soyai*[4,6]	3% GCP 8% NCP *(R)*
Late summer mean ± sd of M1, M4–1, M4–2 and M3–3	Moderate (132) [2]	High[2] 89%	Low (16)	*Phaeocystis* free cells small diatoms Pelagophytes [5]	*Gymnodinium* *Scrippsiella* *Gyrodinium*	*Cymatocylis antarctica, Lohmaniella oviformis*	3.9 ± 1.8% GCP 6.8 ± 2.2% NCP (mean ± sd of M1, M4–1, M4–2) 5.2% GCP 46% NCP *(M3–3)*

1. Christaki et al., 2014; 2. Christaki et al., 2021; 3. Lasbleiz et al., 2016; 4. Georges et al., 2014; 5. Irion et al., 2020; 6. Christaki et al., 2015

[a] Carbon demand is estimated based on biomass, 30% growth efficiency o (Bjørnsen and Kuparinen, 1991; Verity et al., 1993; Neuer and Cowles, 1994; Karayanni et al., 2008) and $\mu = 0.2\ d^{-1}$ corresponding roughly population generation time of about 3 days (Bjørnsen and Kuparinen, 1991; Verity et al., 1993; Neuer and Cowles, 1994; Karayanni et al., 2008).

see also Christaki et al., 2015). *Gymnodinium* can grow in a wide range of environmental conditions due to two particular traits. Their mixotrophy allows them to switch between photosynthesis and grazing depending on present nutrient, prey and light conditions, while they can also feed on a wide range of prey (including other DIN, CIL, and bacteria) (e.g., Strom, 1991; Bockstahler and Coats, 1993; Sherr and Sherr, 2007; Sherr and Sherr, 2007; Jeong et al., 2010, 2018; Lee et al., 2014).

CIL abundances were considerably lower than those of DIN, the median for all stations and seasons being 350 and 1370 cells L^{-1}, respectively (Figs. 4a, c, Fig. 5). DIN can graze on almost all planktonic organisms and are recognized as major microplankton predators (Sherr and Sherr, 2007). In contrast, naked CIL prefer prey of the 5–25 μm size-class (Hansen et al. 1994) and can also feed on bacteria (Sherr et al., 1987; Christaki et al., 1998, 1999). The most abundant CIL during MOBYDICK was *Lohmaniella oviformis* belonging to the <20 μm size class. CIL abundance and biomass were higher after the bloom than during the onset of the bloom. This pattern was likely related to the increase in abundance of their nanophytoplankton preys. However, while pico- and nanophytoplankton increased by about 15-fold between the onset and the post bloom periods in Kerguelen plateau waters (Christaki et al., 2014; Irion et al., 2020), CIL abundance increased only by about 1.4 and 2.5 on- and off-plateau, respectively (Fig. 4c). Also, during MOBYDICK, pico- and nanoplankton showed a 2.6-fold increase between the first and the third visit at M2 (Irion et al., 2020), while CIL slightly decreased (Fig. 4c). The overall CIL abundance was always relatively low and never exceeded 450 cells L^{-1}. The absence of any clear relation between the abundance of CIL and their favorite prey was likely the result of the double top-down control on ciliates by both dinoflagellates and mesozooplankton (Calbet and Saiz, 2005; Franzé and Modigh, 2013). CIL have not been shown to effectively feed on large or chain-forming diatoms (Sherr and Sherr, 2007). Only tintinnid CIL can feed on a large variety of small diatoms (Gowing and Garrison, 1992; Armbrecht et al., 2017). The tintinnids located in the Antarctic zone, delimited by the average location of the Polar Front, contain a large portion of wide-mouthed forms (Dolan et al., 2012). The ability of relatively large tintinnids, in 40–60 μm and 60–100 μm size-classes, to ingest small diatoms is probably an advantage that allows them to form dense populations in SO (e.g., Alder and Boltovskoy, 1991; Buck et al., 1992; Dolan et al., 2012). Indeed, *Cymatocylis antarctica* was the second most abundant CIL and was particularly present at the HNLC M3-station where small diatoms (<20 μm) were also enhanced (*Fragilariopsis, Pseudo-nitzschia, Thalassiosira* and *Chaetoceros,* Irion et al., 2020).

4.3. Potential role of microzooplankton in carbon transfer in planktonic food webs

Comprehensive assessment of grazing in natural phytoplankton communities is still very challenging and relies on many assumptions. One widely used approach is the relatively simple dilution method which estimates grazing rates based on phytoplankton growth in a gradient of grazing pressure. Among the criticisms of the dilution method are that dilution experiments may provide inconsistent results, i.e., abnormally high and/or null grazing rates (e.g., Dolan and McKeon, 2005; Calbet et al., 2011; Calbet and Saiz, 2013). The dilution experiment estimated grazing by the whole heterotrophic community <200 μm, including heterotrophic nanoflagellates. During MOBYDICK, heterotrophic nanoflagellates and their grazing on picoplankton were quantified. The nanoflagellates grazed almost exclusively on heterotrophic bacteria (Christaki et al., 2021). Thus, the high grazing rates measured in the dilution experiments were most likely dominated by microzooplankton grazing. This is in line with the finding that the small sized phytoplankton community was dominated by nano-sized Prymnesiophytes (Irion et al., 2020); and that small phytoplankton cells, which are the preferred microzooplankton prey (prymnesiophytes, prasinophytes and small diatoms), were actively growing (0.22–0.37 division d^{-1}, Irion et al., 2021).

One potential caveat with the dilution experiment is that photoacclimation of phytoplankton to stable light conditions in the incubator may have resulted in reduced Chl *a* concentrations compared to T0 and underestimation of growth rates (Rose et al., 2013).

Another potential caveat with the dilution experiment is reduced phytoplankton growth due to nutrient limitation over the course of the experiment. However, measurements of macro-nutrient concentrations at all stations during the cruise did not suggest any limitations and the noticeable increase in phytoplankton biomass at M2 indicated sufficient iron concentrations even in late summer after the decline of the bloom. Depletion of nutrients to limiting levels over the short duration of the experiments (24 h) was therefore unlikely. The phytoplankton growth rate (μ) and the microzooplankton grazing rate (g) measured during MOBYDICK in the dilution experiments were within the range of previous studies in cold waters (e.g., Menden-Deuer et al., 2018; Schmoker et al., 2013 and references therein). Phytoplankton growth was lower than microzooplankton grazing at all stations (Table 2). Our data add to the surprisingly high variability of estimates of standing stock of phytoplankton grazed by microzooplankton in the Southern Ocean, (from 0 to >100%, median ≈ 50%, Schmoker et al., 2013).

Given the limitations and assumptions of the dilution method, these estimates of phytoplankton consumption by microzooplankton were compared with the CD (Carbon Demand) of DIN and CIL as a proportion of GCP (Gross Community Production) and NCP (Net Community Production). The CD was calculated based on their biomass stocks applying a conservative growth rate $\mu = 0.2\ d^{-1}$ (e.g., Bjørnsen and Kuparinen, 1991; Verity et al., 1993; Neuer and Cowles, 1994; Karayanni et al., 2008; Rose et al., 2013) and a growth efficiency (GE) of 30% (e.g., Straile, 1997; Strom, 1991; Strom and Fredrickson, 2008). According to these estimates, the carbon demand of DIN and CIL accounted for 5 and 3% of the GCP on- and off-plateau, respectively, in late summer. It was, however, considerably higher on the plateau during the onset of the bloom where it accounted for 18% of the GCP (station A3–2, Table 3). The proportion of carbon corresponding to CD changed when NCP (Net Community Production) was taken into account due to the variability in DCR (Dark Community Respiration) among stations. Thus, the amount of NCP needed to cover the DIN + CIL carbon demand varied between 5 and 46% (Table 3). To note, that these estimations of CD and NCP should be considered as conservative since they were based on stocks and literature conversion factors.

The low abundance of microzooplankton despite high grazing rates could also be explained by intra-guild predation which is common for these mixotrophic and heterotrophic organisms (e.g., Franzé and Modigh, 2013) and strong top-down-control through mesozooplankton such as copepods.

In particular, after the end of the bloom (MOBYDICK), the low nutritional quality of phytoplankton probably further enhanced top-down control on microzooplakton by copepods (Sherr and Sherr, 2009; Tsuda et al., 2007). During MOBYDICK, two observations lend support for mesozooplankton top-down control on microzooplankton. First, mesozooplankton abundance showed large variability, ranging between 207 ind. m^{-3} at M2–1 to 1636 ind. m^{-3} at M4–1, and in particular at M2 where it showed a 7-fold increase between the first and the second visit (1473 ind. m^{-3}) at this station. Secondly, grazing experiments showed that there was insignificant grazing of copepods on phytoplankton and that their respiration requirements were never covered by phytoplankton ingestion (Delegrange et al. MOBYDICK unpublished data) suggesting that they were primarily grazing on microzooplankton.

In conclusion, the present study provides two interesting observations: (i) dilution experiments indicated high microzooplankton grazing capacity on phytoplankton; and (ii) microzooplankton biomass remained low, suggesting a top-down feeding impact by copepods. We suggest that DIN and CIL activities, and thus their roles in the trophic web of surface SO waters, are highly dynamic, however, this is not necessarily reflected in their stock variability. Microzooplankton can

apparently not prevent phytoplankton bloom initiations (Sherr and Sherr, 2009), likely due to substantial zooplankton predation on microzooplankton (Stoecker and Capuzzo, 1990). Our observations highlighted the decoupling between microzooplankton stocks (abundance and biomass) and activities (C-transfer) in SO surface waters. Estimations of carbon transfer solely based on microzooplankton stocks will thus likely lead to incorrect results. The strength of the microzooplankton-mesozooplankton relationship is rarely considered in plankton studies (e.g., Froneman et al., 1996; Calbet and Saiz, 2005) and typically neglected in the construction of carbon budgets. The question is therefore: How do we parametrize microzooplankton in ecosystem models? Strom and Fredrickson (2008) recommended to parametrize microzooplankton grazing as a 'sometimes-on, frequently-off' response, rather than a low average. Microzooplankton biomass increases typically during brief periods of time before copepod populations establish, as seen during the onset of the bloom when high DIN biomass was correlated with large diatom grazers on the plateau (Fig. 4, second visit at A3, Christaki et al., 2015). We suggest, that outside this period, when microzooplankton biomass remains low, it continues to play a crucial role as they 'repackage' and 'enrich' phytoplankton carbon for higher trophic levels, and also contribute to nutrient and Fe regeneration (Sarthou et al., 2008).

Supplementary data to this article can be found online at https://doi.org/10.1016/j.jmarsys.2021.103531.

Declaration of Competing Interest

None.

Acknowledgements

We thank B. Quéguiner, the PI of the MOBYDICK project, for providing us the opportunity to participate to this cruise, the captain and crew of the R/V Marion Dufresne for their enthusiasm and support aboard during the MOBYDICK–THEMISTO cruise (10.17600/18000403) and the chief scientist I. Obernosterer. This work was supported by the French oceanographic fleet ("Flotte océanographique française"), the French ANR ("Agence Nationale de la Recherche", AAPG 2017 program, MOBYDICK Project number: ANR-17-01-0013CE), and the French Research program of INSU-CNRS LEFE/CYBER ("Les enveloppes fluides et l'environnement" – "Cycles biogéochimiques, environnement et ressources"). This work was also supported by ULCO (Université du Littoral), CPER MARCO (https://marco.univ-littoral.fr/), the Region "Hauts de France" and CNRS LEFE-EC2CO through the project PLANKTON-PARTY. *The authors clearly state there is no conflict of interests regarding this paper.*

Author contribution

UC: designed the study, carried out field work, analyzed data and wrote the paper with the help of all the co-authors. I-D S: analyzed microscopy samples, prepared data. AD analyzed dilution samples, analyzed dilution data. SI: analyzed molecular and pigment data. LC: analyzed microscopy samples. LJ: offered critical reading and comments. IS: carried out field work, analyzed molecular data.

References

Alder, V.A., Boltovskoy, D., 1991. Microplanktonic distributional patterns west of the Antarctic Peninsula, with special emphasis on the Tintinnids. Polar Biol. 11, 103–112. https://doi.org/10.1007/BF00234272.

Armand, L.K., Cornet-Barthaux, V., Mosseri, J., Quéguiner, B., 2008. Late summer diatom biomass and community structure on and around the naturally iron-fertilised Kerguelen Plateau in the Southern Ocean. Deep-Sea Res. II Top. Stud. Oceanogr. 55, 653–676. https://doi.org/10.1016/j.dsr2.2007.12.031.

Armbrecht, L.H., Eriksen, R., Leventer, A., Armand, L.K., 2017. First observations of living sea-ice diatom agglomeration to tintinnid loricae in East Antarctica. J. Plankton Res. 39, 795–802. https://doi.org/10.1093/plankt/fbx036.

Bachy, C., Dolan, J.R., López-García, P., Deschamps, P., Moreira, D., 2013. Accuracy of protist diversity assessments: morphology compared with cloning and direct pyrosequencing of 18S rRNA genes and ITS regions using the conspicuous tintinnid ciliates as a case study. ISME J. 7, 244–255. https://doi.org/10.1038/ismej.2012.106.

Bik, H.M., Porazinska, D.L., Creer, S., Caporaso, J.G., Knight, R., Thomas, W.K., 2012. Sequencing our way towards understanding global eukaryotic biodiversity. Trends Ecol. Evol. 27, 233–243. https://doi.org/10.1016/j.tree.2011.11.010.

Bjørnsen, P.K., Kuparinen, J., 1991. Growth and herbivory by heterotrophic dinoflagellates in the Southern Ocean, studied by microcosm experiments. Mar. Biol. 109, 397–405. https://doi.org/10.1007/BF01313505.

Blain, S., Quéguiner, B., Armand, L., Belviso, S., Bombled, B., Bopp, L., Bowie, A., Brunet, C., Brussaard, C., Carlotti, F., Christaki, U., Corbière, A., Durand, I., Ebersbach, F., Fuda, J.-L., Garcia, N., Gerringa, L., Griffiths, B., Guigue, C., Guillerm, C., Jacquet, S., Jeandel, C., Laan, P., Lefèvre, D., Lo Monaco, C., Malits, A., Mosseri, J., Obernosterer, I., Park, Y.-H., Picheral, M., Pondaven, P., Remenyi, T., Sandroni, V., Sarthou, G., Savoye, N., Scouarnec, L., Souhaut, M., Thuiller, D., Timmermans, K., Trull, T., Uitz, J., van Beek, P., Veldhuis, M., Vincent, D., Viollier, E., Vong, L., Wagener, T., 2007. Effect of natural iron fertilization on carbon sequestration in the Southern Ocean. Nature 446, 1070–1074. https://doi.org/10.1038/nature05700.

Blain, S., Capparos, J., Guéneuguès, A., Obernosterer, I., Oriol, L., 2015. Distributions and stoichiometry of dissolved nitrogen and phosphorus in the iron-fertilized region near Kerguelen (Southern Ocean). Biogeosciences 12, 623–635. https://doi.org/10.5194/bg-12-623-2015.

Bockstahler, K.R., Coats, D.W., 1993. Grazing of the mixotrophic dinoflagellate *Gymnodinium sanguineum* on ciliate populations of Chesapeake Bay. Mar. Biol. 116, 477–487. https://doi.org/10.1007/BF00350065.

Bower, S.M., Carnegie, R.B., Goh, B., Jones, S.R.M., Lowe, G.J., Mak, M.W.S., 2004. Preferential PCR amplification of parasitic protistan small subunit rDNA from metazoan tissues. J. Eukaryotic Microbiol. 51, 325–332. https://doi.org/10.1111/j.1550-7408.2004.tb00574.x.

Brussaard, C.P.D., Timmermans, K.R., Uitz, J., Veldhuis, M.J.W., 2008. Virioplankton dynamics and virally induced phytoplankton lysis versus microzooplankton grazing southeast of the Kerguelen (Southern Ocean). Deep Sea Res. II 44, 752–765. https://doi.org/10.1016/j.dsr2.2007.12.034.

Buck, K.R., Garrison, D.L., Hopkins, T.L., 1992. Abundance and distribution of tintinnid ciliates in an ice edge zone during the austral autumn. Antartic Sci. 4, 3–8. https://doi.org/10.1017/S0954102092000038.

Calbet, A., Landry, M.R., 2004. Phytoplankton growth, microzooplankton grazing, and carbon cycling in marine systems. Limnol. Oceanogr. 49, 51–57. https://doi.org/10.4319/lo.2004.49.1.0051.

Calbet, A., Saiz, E., 2005. The ciliate-copepod link in marine ecosystems. Aquat. Microb. Ecol. 38, 157–167. https://doi.org/10.3354/ame038157.

Calbet, A., Saiz, E., 2013. Effects of trophic cascades in dilution grazing experiments: from artificial saturated feeding responses to positive slopes. J. Plankton Res. 35, 1183–1191. https://doi.org/10.1093/plankt/fbt067.

Calbet, A., Saiz, E., Almeda, R., Movilla, J.I., Alcaraz, M., 2011. Low microzooplankton grazing rates in the Arctic Ocean during a *Phaeocystis pouchetii* bloom (Summer 2007): fact or artifact of the dilution technique? J. Plankton Res. 33, 687–701. https://doi.org/10.1093/plankt/fbq142.

Callahan, B.J., McMurdie, P.J., Rosen, M.J., Han, A.W., Johnson, A.J.A., Holmes, S.P., 2016. DADA2: high-resolution sample inference from illumina amplicon data. Nat. Methods 13, 581–583. https://doi.org/10.1038/nmeth.3869.

Campbell, R.G., Sherr, E.B., Ashjian, C.J., Plourde, S., Sherr, B.F., Hill, V., Stockwell, D. A., 2009. Mesozooplankton prey preference and grazing impact in the western Arctic Ocean. Deep-Sea Res. II Top. Stud. Oceanogr. 56, 1274–1289. https://doi.org/10.1016/j.dsr2.2008.10.027.

Capella-Gutierrez, S., Silla-Martinez, J.M., Gabaldon, T., 2009. trimAl: a tool for automated alignment trimming in large-scale phylogenetic analyses. Bioinformatics 25, 1972–1973. https://doi.org/10.1093/bioinformatics/btp348.

Caporaso, J.G., Kuczynski, J., Stombaugh, J., Bittinger, K., Bushman, F.D., Costello, E.K., Fierer, N., Peña, A.G., Goodrich, J.K., Gordon, J.I., Huttley, G.A., Kelley, S.T., Knights, D., Koenig, J.E., Ley, R.E., Lozupone, C.A., McDonald, D., Muegge, B.D., Pirrung, M., Reeder, J., Sevinsky, J.R., Turnbaugh, P.J., Walters, W.A., Widmann, J., Yatsunenko, T., Zaneveld, J., Knight, R., 2010. QIIME allows analysis of high-throughput community sequencing data. Nat. Methods 7, 335–336. https://doi.org/10.1038/nmeth.f.303.

Caron, D.A., Hutchins, D.A., 2013. The effects of changing climate on microzooplankton grazing and community structure: drivers, predictions and knowledge gaps. J. Plankton Res. 35, 235–252. https://doi.org/10.1093/plankt/fbs091.

Caron, D.A., Dennett, M.R., Lonsdale, D.J., Moran, D.M., Shalapyonok, L., 2000. Microzooplankton herbivory in the Ross Sea, Antarctica. Deep-Sea Res. II Top. Stud. Oceanogr. 47, 3249–3272. https://doi.org/10.1016/S0967-0645(00)00067-9.

Caron, D.A., Worden, A.Z., Countway, P.D., Demir, E., Heidelberg, K.B., 2009. Protists are microbes too: a perspective. ISME J. 3, 4–12. https://doi.org/10.1038/ismej.2008.101.

Caron, D.A., Countway, P.D., Jones, A.C., Kim, D.Y., Schnetzer, A., 2012. Marine protistan diversity. Annu. Rev. Mar. Sci. 4, 467–493. https://doi.org/10.1146/annurev-marine-120709-142802.

Cavagna, A.J., Fripiat, F., Elskens, M., Dehairs, F., Mangion, P., Chirurgien, L., Closset, I., Lasbleiz, M., Flores-Leiva, L., Cardinal, D., Leblanc, K., Fernandez, C., Lefèvre, D., Oriol, L., Blain, S., Quéguiner, B., 2014. Biological productivity regime and associated N cycling in the vicinity of Kerguelen Island area, Southern Ocean. Biogeosci. Discuss. 11, 18073–18104. https://doi.org/10.5194/bgd-11-18073-2014.

Cavagna, A.J., Fripiat, F., Elskens, M., Mangion, P., Chirurgien, L., Closset, I., Lasbleiz, M., Florez-Leiva, L., Cardinal, D., Leblanc, K., Fernandez, C., Lefèvre, D., Oriol, L., Blain, S., Quéguiner, B., Dehairs, F., 2015. Production regime and associated N cycling in the vicinity of Kerguelen Island, Southern Ocean. Biogeosciences 12, 6515–6528. https://doi.org/10.5194/bg-12-6515-2015.

Charvet, S., Vincent, W.F., Lovejoy, C., 2012. Chrysophytes and other protists in high Arctic lakes: molecular gene surveys, pigment signatures and microscopy. Polar Biol. 35, 733–748. https://doi.org/10.1007/s00300-011-1118-7.

Chen, B., Landry, M.R., Huang, B., Liu, H., 2012. Does warming enhance the effect of microzooplankton grazing on marine phytoplankton in the ocean? Limnol. Oceanogr. 57, 519–526. https://doi.org/10.4319/lo.2012.57.2.0519.

Christaki, U., Dolan, J.R., Pelegri, S., Rassoulzadegan, F., 1998. Consumption of picoplankton-size particles by marine ciliates: effects of physiological state of the ciliate and particle quality. Limnol. Oceanogr. 43, 458–464. https://doi.org/10.4319/lo.1998.43.3.0458.

Christaki, U., Jacquet, S., Dolan, J.R., Vaulot, D., Rassoulzadegan, F., 1999. Growth and grazing on Prochlorococcus and Synechococcus by two marine ciliates. Limnol. Oceanogr. 44, 52–61. https://doi.org/10.4319/lo.1999.44.1.0052.

Christaki, U., Obernosterer, I., Van Wambeke, F., Veldhuis, M., Garcia, N., Catala, P., 2008. Microbial food web structure in a naturally iron-fertilized area in the Southern Ocean (Kerguelen Plateau). Deep-Sea Res. II Top. Stud. Oceanogr. 55, 706–719. https://doi.org/10.1016/j.dsr2.2007.12.009.

Christaki, U., Lefèvre, D., Georges, C., Colombet, J., Catala, P., Courties, C., Sime-Ngando, T., Blain, S., Obernosterer, I., 2014. Microbial food web dynamics during spring phytoplankton blooms in the naturally iron-fertilized Kerguelen area (Southern Ocean). Biogeosciences 11, 6739–6753. https://doi.org/10.5194/bg-11-6739-2014.

Christaki, U., Georges, C., Genitsaris, S., Monchy, S., 2015. Microzooplankton community associated with phytoplankton blooms in the naturally iron-fertilized Kerguelen area (Southern Ocean). FEMS Microbiol. Ecol. 91 https://doi.org/10.1093/femsec/fiv068.

Christaki, U., Guenegues, A., Liu, Y., Blain, S., Catala, C., Colombet, J., Debeljak, P., Jardillier, L., Irion, S., Planchon, F., Sassenhagen, I., Sime-Ngando, T., Ingrid Obernosterer, I., 2021. Seasonal microbial food web dynamics in contrasting Southern Ocean productivity regimes. Limnol. Oceanogr. https://doi.org/10.1002/lno.11591 lno.11591.

Closset, I., Lasbleiz, M., Leblanc, K., Quéguiner, B., Cavagna, A.-J., Elskens, M., Navez, J., Cardinal, D., 2014. Seasonal evolution of net and regenerated silica production around a natural Fe-fertilized area in the Southern Ocean estimated with Si isotopic approaches. Biogeosciences 11, 5827–5846. https://doi.org/10.5194/bg-11-5827-2014.

Daugbjerg, N., Hansen, G., Larsen, J., Moestrup, Ø., 2000. Phylogeny of some of the major genera of dinoflagellates based on ultrastructure and partial LSU rDNA sequence data, including the erection of three new genera of unarmoured dinoflagellates. Phycologia 39, 302–317. https://doi.org/10.2216/i0031-8884-39-4-302.1.

Dolan, J.R., McKeon, K., 2005. The reliability of grazing rate estimates from dilution experiments: have we over-estimated rates of organic carbon consumption by microzooplankton? Ocean Sci. 1, 1–7. https://doi.org/10.5194/os-1-1-2005.

Dolan, J.R., Pierce, R.W., Yang, E.J., Kim, S.Y., 2012. Southern Ocean biogeography of tintinnid ciliates of the marine plankton. J. Eukaryot. Microbiol. 59, 511–519. https://doi.org/10.1111/j.1550-7408.2012.00646.x.

Doledec, S., Chessel, D., 1994. Co-inertia analysis: an alternative method for studying species-environment relationships. Freshw. Biol. 31, 277–294. https://doi.org/10.1111/j.1365-2427.1994.tb01741.x.

Dray, S., Dufour, A.-B., 2007. The ade4 package: implementing the duality diagram for ecologists. J. Stat. Soft. 22 https://doi.org/10.18637/jss.v022.i04.

Dray, S., Chessel, D., Thioulouse, J., 2003. Co-inertia analysis and the linking of ecological data tables. Ecology 84, 3078–3089. https://doi.org/10.1890/03-0178.

Edgar, R.C., 2004. MUSCLE: multiple sequence alignment with high accuracy and high throughput. Nucleic Acids Res. 32, 1792–1797. https://doi.org/10.1093/nar/gkh340.

Franzé, G., Modigh, M., 2013. Experimental evidence for internal predation in microzooplankton communities. Mar. Biol. 160, 3103–3112. https://doi.org/10.1007/s00227-013-2298-1.

Froneman, P., Pakhomov, E., Perissinotto, R., McQuaid, C., 1996. Role of microplankton in the diet and daily ration of Antarctic zooplankton species during austral summer. Mar. Ecol. Prog. Ser. 143, 15–23. https://doi.org/10.3354/meps143015.

Georges, C., Monchy, S., Genitsaris, S., Christaki, U., 2014. Protist community composition during early phytoplankton blooms in the naturally iron-fertilized Kerguelen area (Southern Ocean). Biogeosciences 11, 5847–5863. https://doi.org/10.5194/bg-11-5847-2014.

Gowing, M.M., Garrison, D.L., 1992. Abundance and feeding ecology of larger protozooplankton in the ice edge zone of the Weddell and Scotia seas during the austral winter. Deep Sea Res. Part A. Oceanogr. Res. Papers 39, 893–919. https://doi.org/10.1016/0198-0149(92)90128-G.

Grattepanche, J.-D., Breton, E., Brylinski, J.-M., Lecuyer, E., Christaki, U., 2011a. Succession of primary producers and micrograzers in a coastal ecosystem dominated by *Phaeocystis globosa* blooms. J. Plankton Res. 33, 37–50. https://doi.org/10.1093/plankt/fbq097.

Grattepanche, J.-D., Vincent, D., Breton, E., Christaki, U., 2011b. Microzooplankton herbivory during the diatom–Phaeocystis spring succession in the eastern English Channel. J. Exp. Mar. Biol. Ecol. 404, 87–97. https://doi.org/10.1016/j.jembe.2011.04.004.

Guidi, L., Chaffron, S., Bittner, L., Eveillard, D., Larhlimi, A., Roux, S., Darzi, Y., Audic, S., Berline, L., Brum, J.R., Coelho, L.P., Espinoza, J.C.I., Malviya, S., Sunagawa, S., Dimier, C., Kandels-Lewis, S., Picheral, M., Poulain, J., Searson, S., Stemmann, L., Not, F., Hingamp, P., Speich, S., Follows, M., Karp-Boss, L., Boss, E., Ogata, H., Pesant, S., Weissenbach, J., Wincker, P., Acinas, S.G., Bork, P., de Vargas, C., Iudicone, D., Sullivan, M.B., Raes, J., Karsenti, E., Bowler, C., Gorsky, G., 2016. Plankton networks driving carbon export in the oligotrophic ocean. Nature 532, 465–470. https://doi.org/10.1038/nature16942.

Guillou, L., Bachar, D., Audic, S., Bass, D., Berney, C., Bittner, L., Boutte, C., Burgaud, G., de Vargas, C., Decelle, J., del Campo, J., Dolan, J.R., Dunthorn, M., Edvardsen, B., Holzmann, M., Kooistra, W.H.C.F., Lara, E., Le Bescot, N., Logares, R., Mahé, F., Massana, R., Montresor, M., Morard, R., Not, F., Pawlowski, J., Probert, I., Sauvadet, A.-L., Siano, R., Stoeck, T., Vaulot, D., Zimmermann, P., Christen, R., 2012. The protist ribosomal reference database (PR2): a catalog of unicellular eukaryote small sub-unit rRNA sequences with curated taxonomy. Nucleic Acids Res. 41, D597–D604. https://doi.org/10.1093/nar/gks1160.

Hall, J.A., Safi, K., 2001. The impact of in situ Fe fertilisation on the microbial food web in the Southern Ocean. Deep-Sea Res. II Top. Stud. Oceanogr. 48, 2591–2613. https://doi.org/10.1016/S0967-0645(01)00010-8.

Henjes, J., Assmy, P., Klaas, C., Verity, P., Smetacek, V., 2007. Response of microzooplankton (protists and small copepods) to an iron-induced phytoplankton bloom in the Southern Ocean (EisenEx). Deep-Sea Res. I Oceanogr. Res. Pap. 54, 363–384. https://doi.org/10.1016/j.dsr.2006.12.004.

Irigoien, X., Flynn, K.J., Harris, R.P., 2005. Phytoplankton blooms: a 'loophole' in microzooplankton grazing impact? J. Plankton Res. 27, 313–321. https://doi.org/10.1093/plankt/fbi011.

Irion, S., Jardillier, L., Sassenhagen, I., Christaki, U., 2020. Marked spatio-temporal variations in small phytoplankton structure in contrasted waters of the Southern Ocean (Kerguelen area). Limnol. Oceanogr. https://doi.org/10.1002/lno.11555 lno.11555.

Irion, S., Christaki, U., Berthelot, U., L'Helghen, S., Jardillier, L., 2021. Small phytoplankton contribute greatly to CO2-fixation after the diatom bloom in the Southern Ocean 2021. ISME J. https://doi.org/10.1038/s41396-021-00915-z.

Jeong, H.J., Yoo, Y.D., Kim, J.S., Seong, K.A., Kang, N.S., Kim, T.H., 2010. Growth, feeding and ecological roles of the mixotrophic and heterotrophic dinoflagellates in marine planktonic food webs. Ocean Sci. J. 45, 65–91. https://doi.org/10.1007/s12601-010-0007-2.

Jeong, H.J., You, J.H., Lee, K.H., Kim, S.J., Lee, S.Y., 2018. Feeding by common heterotrophic protists on the mixotrophic alga *Gymnodinium smaydae* (Dinophyceae), one of the fastest growing dinoflagellates. J. Phycol. 54, 734–743. https://doi.org/10.1111/jpy.12775.

Karayanni, H., Christaki, U., Van Wambeke, F., Thyssen, M., Denis, M., 2008. Heterotrophic nanoflagellate and ciliate bacterivorous activity and growth in the northeast Atlantic Ocean: a seasonal mesoscale study. Aquat. Microb. Ecol. 51, 169–181. https://doi.org/10.3354/ame01181.

Kenkel, N.C., 2006. On selecting an appropriate multivariate analysis. Can. J. Plant Sci. 86, 663–676. https://doi.org/10.4141/P05-164.

Kiørboe, T., Visser, A., 1999. Predator and prey perception in copepods due to hydromechanical signals. Mar. Ecol. Prog. Ser. 179, 81–95. https://doi.org/10.3354/meps179081.

Kofoid, C.A., Campbell, A.S., 1929. A Conspectus of the Marine and Freshwater Ciliata Belonging to the suborder Tintinnoinea, with Despcriptions of New Species Principally from the Agassiz Expedition to the Eastern Tropical Pacific 1904-1905. University of California Publications in Zoology, Berkley, Calif, p. 403.

Landry, M.R., Hassett, R.P., 1982. Estimating the grazing impact of marine micro-zooplankton. Mar. Biol. 67, 283–288. https://doi.org/10.1007/BF00397668.

Lasbleiz, M., Leblanc, K., Blain, S., Ras, J., Cornet-Barthaux, V., Hélias Nunige, S., Quéguiner, B., 2014. Pigments, elemental composition (C, N, P, and Si), and stoichiometry of particulate matter in the naturally iron fertilized region of Kerguelen in the Southern Ocean. Biogeosciences 11, 5931–5955. https://doi.org/10.5194/bg-11-5931-2014.

Lasbleiz, M., Leblanc, K., Armand, L.K., Christaki, U., Georges, C., Obernosterer, I., Quéguiner, B., 2016. Composition of diatom communities and their contribution to plankton biomass in the naturally iron-fertilized region of Kerguelen in the Southern Ocean. FEMS Microbiol. Ecol. 92. https://doi.org/10.1093/femsec/fiw171.

Lawerence, C., Menden-Deuer, S., 2012. Drivers of protistan grazing pressure: seasonal signals of plankton community composition and environmental conditions. Mar. Ecol. Prog. Ser. 459, 39–52. https://doi.org/10.3354/meps09771.

Lê, S., Josse, J., Husson, F., 2008. FactoMineR : an *R* package for multivariate analysis. J. Stat. Soft. 25 https://doi.org/10.18637/jss.v025.i01.

Lee, K.H., Jeong, H.J., Jang, T.Y., Lim, A.S., Kang, N.S., Kim, J.-H., Kim, K.Y., Park, K.-T., Lee, K., 2014. Feeding by the newly described mixotrophic dinoflagellate *Gymnodinium smaydae*: feeding mechanism, prey species, and effect of prey concentration. J. Exp. Mar. Biol. Ecol. 459, 114–125. https://doi.org/10.1016/j.jembe.2014.05.011.

Letunic, I., Bork, P., 2016. Interactive tree of life (iTOL) v3: an online tool for the display and annotation of phylogenetic and other trees. Nucleic Acids Res. 44, W242–W245. https://doi.org/10.1093/nar/gkw290.

Lynn, D.H., Montagnes, D.J.S., 1988. Taxonomic descriptions of some conspicuous species of *Strobilidiine ciliates* (Ciliophora: Choreotrichida) from the Isles of Shoals, Gulf of Maine. J. Mar. Biol. Assoc. U. K. 68, 639–658. https://doi.org/10.1017/S0025315400028770.

Mackey, M., Mackey, D., Higgins, H., Wright, S., 1996. CHEMTAX - a program for estimating class abundances from chemical markers:application to HPLC measurements of phytoplankton. Mar. Ecol. Prog. Ser. 144, 265–283. https://doi.org/10.3354/meps144265.

McMinn, A., Scot, F.J., 2005. Dinoflagellates. In: Scott, F.J., Marchant, H.W. (Eds.), Antarctic Marine Protists. ABRS and AAD Publishers, Canberra, pp. 202–250.

McMurdie, P.J., Holmes, S., 2013. Phyloseq: an R package for reproducible interactive analysis and graphics of microbiome census data. PLoS ONE 8, e61217. https://doi.org/10.1371/journal.pone.0061217.
Medinger, R., Nolte, V., Pandey, R.V., Jost, S., Ottenwälder, B., Schlötterer, C., Boenigk, J., 2010. Diversity in a hidden world: potential and limitation of next-generation sequencing for surveys of molecular diversity of eukaryotic microorganisms. Mol. Ecol. 19, 32–40. https://doi.org/10.1111/j.1365-294X.2009.04478.x.
Menden-Deuer, S., Lessard, E.J., 2000. Carbon to volume relationships for dinoflagellates, diatoms, and other protist plankton. Limnol. Oceanogr. 45, 569–579. https://doi.org/10.4319/lo.2000.45.3.0569.
Menden-Deuer, S., Lawrence, C., Franzè, G., 2018. Herbivorous protist growth and grazing rates at in situ and artificially elevated temperatures during an Arctic phytoplankton spring bloom. PeerJ 6, e5264. https://doi.org/10.7717/peerj.5264.
Mordret, S., Piredda, R., Vaulot, D., Montresor, M., Kooistra, W.H.C.F., Sarno, D., 2018. DINOREF: a curated dinoflagellate (Dinophyceae) reference database for the 18S rRNA gene. Mol. Ecol. Resour. 18, 974–987. https://doi.org/10.1111/1755-0998.12781.
Morison, F., Menden-Deuer, S., 2018. Seasonal similarity in rates of protistan herbivory in fjords along the Western Antarctic Peninsula. Limnol. Oceanogr. 63, 2858–2876. https://doi.org/10.1002/lno.11014.
Mosseri, J., Quéguiner, B., Armand, L., Cornet-Barthaux, V., 2008. Impact of iron on silicon utilization by diatoms in the Southern Ocean: a case study of Si/N cycle decoupling in a naturally iron-enriched area. Deep-Sea Res. II Top. Stud. Oceanogr. 55, 801–819. https://doi.org/10.1016/j.dsr2.2007.12.003.
Neuer, S., Cowles, T., 1994. Protist herbivory in the Oregon upwelling system. Mar. Ecol. Prog. Ser. 113, 147–162. https://doi.org/10.3354/meps113147.
Obiol, A., Giner, C.R., Sánchez, P., Duarte, C.M., Acinas, S.G., Massana, R., 2020. A metagenomic assessment of microbial eukaryotic diversity in the global ocean. Mol. Ecol. Resour. 20, 1755–0998.13147. https://doi.org/10.1111/1755-0998.13147.
Pawlowski, J., Audic, S., Adl, S., Bass, D., Belbahri, L., Berney, C., Bowser, S.S., Cepicka, I., Decelle, J., Dunthorn, M., Fiore-Donno, A.M., Gile, G.H., Holzmann, M., Jahn, R., Jirků, M., Keeling, P.J., Kostka, M., Kudryavtsev, A., Lara, E., Lukeš, J., Mann, D.G., Mitchell, E.A.D., Nitsche, F., Romeralo, M., Saunders, G.W., Simpson, A. G.B., Smirnov, A.V., Spouge, J.L., Stern, R.F., Stoeck, T., Zimmermann, J., Schindel, D., de Vargas, C., 2012. CBOL protist working group: barcoding eukaryotic richness beyond the animal, plant, and fungal kingdoms. PLoS Biol. 10, e1001419 https://doi.org/10.1371/journal.pbio.1001419.
Petz, W., 2005. Ciliates. In: Scott, F.J., Marchant, H.J. (Eds.), Antarctic Marine Protists. ABRS and AAD Publishers, Canberra, p. 563.
Pollard, R., Sanders, R., Lucas, M., Statham, P., 2007. The Crozet natural iron bloom and export experiment (CROZEX). Deep-Sea Res. II Top. Stud. Oceanogr. 54, 1905–1914. https://doi.org/10.1016/j.dsr2.2007.07.023.
Pollard, R.T., Salter, I., Sanders, R.J., Lucas, M.I., Moore, C.M., Mills, R.A., Statham, P.J., Allen, J.T., Baker, A.R., Bakker, D.C.E., Charette, M.A., Fielding, S., Fones, G.R., French, M., Hickman, A.E., Holland, R.J., Hughes, J.A., Jickells, T.D., Lampitt, R.S., Morris, P.J., Nédélec, F.H., Nielsdóttir, M., Planquette, H., Popova, E.E., Poulton, A. J., Read, J.F., Seeyave, S., Smith, T., Stinchcombe, M., Taylor, S., Thomalla, S., Venables, H.J., Williamson, R., Zubkov, M.V., 2009. Southern Ocean deep-water carbon export enhanced by natural iron fertilization. Nature 457, 577–580. https://doi.org/10.1038/nature07716.
Poulton, A.J., Mark Moore, C., Seeyave, S., Lucas, M.I., Fielding, S., Ward, P., 2007. Phytoplankton community composition around the Crozet Plateau, with emphasis on diatoms and phaeocystis. Deep-Sea Res. II Top. Stud. Oceanogr. 54, 2085–2105. https://doi.org/10.1016/j.dsr2.2007.06.005.
Putt, M., Stoecker, D.K., 1989. An experimentally determined carbon : volume ratio for marine “oligotrichous” ciliates from estuarine and coastal waters. Limnol. Oceanogr. 34, 1097–1103. https://doi.org/10.4319/lo.1989.34.6.1097.
Quéguiner, B., 2013. Iron fertilization and the structure of planktonic communities in high nutrient regions of the Southern Ocean. Deep-Sea Res. II Top. Stud. Oceanogr. 90, 43–54. https://doi.org/10.1016/j.dsr2.2012.07.024.
Ras, J., Claustre, H., Uitz, J., 2008. Spatial variability of phytoplankton pigment distributions in the subtropical South Pacific Ocean: comparison between in situ and predicted data. Biogeosciences 5, 353–369. https://doi.org/10.5194/bg-5-353-2008.
Rose, J.M., Fitzpatrick, E., Wang, A., Gast, R.J., Caron, D.A., 2013. Low temperature constrains growth rates but not short-term ingestion rates of Antarctic ciliates. Polar Biol. 36, 645–659. https://doi.org/10.1007/s00300-013-1291-y.
Saito, H., Suzuki, K., Hinuma, A., Ota, T., Fukami, K., Kiyosawa, H., Saino, T., Tsuda, A., 2005. Responses of microzooplankton to in situ iron fertilization in the western subarctic Pacific (SEEDS). Prog. Oceanogr. 64, 223–236. https://doi.org/10.1016/j.pocean.2005.02.010.
Saito, H., Ota, T., Suzuki, K., Nishioka, J., Tsuda, A., 2006. Role of heterotrophic dinoflagellate *Gyrodinium* sp. in the fate of an iron induced diatom bloom. Geophys. Res. Lett. 33, L09602 https://doi.org/10.1029/2005GL025366.
Sarthou, G., Vincent, D., Christaki, U., Obernosterer, I., Timmermans, K.R., Brussaard, C. P.D., 2008. The fate of biogenic iron during a phytoplankton bloom induced by natural fertilisation: impact of copepod grazing. Deep-Sea Res. II Top. Stud. Oceanogr. 55, 734–751. https://doi.org/10.1016/j.dsr2.2007.12.033.
Sassenhagen, I., Irion, S., Jardillier, L., Moreira, D., Christaki, U., 2020. Protist interactions and community structure during early autumn in the Kerguelen region (Southern Ocean). Protist 171, 125709. https://doi.org/10.1016/j.protis.2019.125709.
Schiller, J., 1931–1937. Dinoflagellatae (Peridinineae) in monographischer Behandlung. In: Rabenhorst, L. (Ed.), Kryptogamen-Flora von Deutschland, Österreichs und der Schweiz. Akad. Verlag, Leipzig. Vol. 10 (3): Teil 1 (1–3) (1931–1933): Teil 2 (1–4) (1935–1937).
Schmoker, C., Hernández-León, S., Calbet, A., 2013. Microzooplankton grazing in the oceans: impacts, data variability, knowledge gaps and future directions. J. Plankton Res. 35, 691–706. https://doi.org/10.1093/plankt/fbt023.
Sherr, E., Sherr, B., 2007. Heterotrophic dinoflagellates: a significant component of microzooplankton biomass and major grazers of diatoms in the sea. Mar. Ecol. Prog. Ser. 352, 187–197. https://doi.org/10.3354/meps07161.
Sherr, E., Sherr, B., 2009. Capacity of herbivorous protists to control initiation and development of mass phytoplankton blooms. Aquat. Microb. Ecol. 57, 253–262. https://doi.org/10.3354/ame01358.
Sherr, B.F., Sherr, E.B., Fallon, R.D., 1987. Use of monodispersed, fluorescently labeled bacteria to estimate in situ protozoan bacterivoryt. Appl. Environ. Microbiol. 53, 958–965.
Smetacek, V., Assmy, P., Henjes, J., 2004. The role of grazing in structuring Southern Ocean pelagic ecosystems and biogeochemical cycles. Antartic Sci. 16, 541–558. https://doi.org/10.1017/S0954102004002317.
Stamatakis, A., 2014. RAxML version 8: a tool for phylogenetic analysis and post-analysis of large phylogenies. Bioinformatics 30, 1312–1313. https://doi.org/10.1093/bioinformatics/btu033.
Steinberg, D.K., Landry, M.R., 2017. Zooplankton and the ocean carbon cycle. Annu. Rev. Mar. Sci. 9, 413–444. https://doi.org/10.1146/annurev-marine-010814-015924.
Stern, R., Kraberg, A., Bresnan, E., Kooistra, W.H.C.F., Lovejoy, C., Montresor, M., Morán, X.A.G., Not, F., Salas, R., Siano, R., Vaulot, D., Amaral-Zettler, L., Zingone, A., Metfies, K., 2018. Molecular analyses of protists in long-term observation programmes—current status and future perspectives. J. Plankton Res. 40, 519–536. https://doi.org/10.1093/plankt/fby035.
Stoecker, D.K., Capuzzo, J.M., 1990. Predation on protozoa: its importance to zooplankton. J. Plankton Res. 12, 891–908. https://doi.org/10.1093/plankt/12.5.891.
Straile, D., 1997. Gross growth efficiencies of protozoan and metazoan zooplankton and their dependence on food concentration, predator-prey weight ratio, and taxonomic group. Limnol. Oceanogr. 42, 1375–1385. https://doi.org/10.4319/lo.1997.42.6.1375.
Strom, S., 1991. Growth and grazing rates of the herbivorous dinoflagellate Gymnodinium sp. from the open subarctic Pacific Ocean. Mar. Ecol. Prog. Ser. 78, 103–113. https://doi.org/10.3354/meps078103.
Strom, S.L., Fredrickson, K.A., 2008. Intense stratification leads to phytoplankton nutrient limitation and reduced microzooplankton grazing in the southeastern Bering Sea. Deep-Sea Res. II Top. Stud. Oceanogr. 55, 1761–1774. https://doi.org/10.1016/j.dsr2.2008.04.008.
Tomas, C.R., 1997. Identifying Marine Phytoplankton. Elsevier, London, p. 858.
Tsuda, A., Takeda, S., Saito, H., Nishioka, J., Kudo, I., Nojiri, Y., Suzuki, K., Uematsu, M., Wells, M.L., Tsumune, D., Yoshimura, T., Aono, T., Aramaki, T., Cochlan, W.P., Hayakawa, M., Imai, K., Isada, T., Iwamoto, Y., Johnson, W.K., Kameyama, S., Kato, S., Kiyosawa, H., Kondo, Y., Levasseur, M., Machida, R.J., Nagao, I., Nakagawa, F., Nakanishi, T., Nakatsuka, S., Narita, A., Noiri, Y., Obata, H., Ogawa, H., Oguma, K., Ono, T., Sakuragi, T., Sasakawa, M., Sato, M., Shimamoto, A., Takata, H., Trick, C.G., Watanabe, Y.W., Wong, C.S., Yoshie, N., 2007. Evidence for the grazing hypothesis: grazing reduces phytoplankton responses of the HNLC ecosystem to iron enrichment in the western subarctic pacific (SEEDS II). J. Oceanogr. 63, 983–994. https://doi.org/10.1007/s10872-007-0082-x.
Uitz, J., Claustre, H., Griffiths, F.B., Ras, J., Garcia, N., Sandroni, V., 2009. A phytoplankton class-specific primary production model applied to the Kerguelen Islands region (Southern Ocean). Deep-Sea Res. I Oceanogr. Res. Pap. 56, 541–560. https://doi.org/10.1016/j.dsr.2008.11.006.
Vargas, C., González, H., 2004. Plankton community structure and carbon cycling in a coastal upwelling system. I. Bacteria, microprotozoans and phytoplankton in the diet of copepods and appendicularians. Aquat. Microb. Ecol. 34, 151–164. https://doi.org/10.3354/ame034151.
Verity, P.G., Stoecker, D.K., Sieracki, M.E., Nelson, J.R., 1993. Grazing, growth and mortality of microzooplankton during the 1989 North Atlantic spring bloom at 47°N, 18°W. Deep-Sea Res. I Oceanogr. Res. Pap. 40, 1793–1814. https://doi.org/10.1016/0967-0637(93)90033-Y.
Wolf, C., Frickenhaus, S., Kilias, E.S., Peeken, I., Metfies, K., 2014. Protist community composition in the Pacific sector of the Southern Ocean during austral summer 2010. Polar Biol. 37, 375–389. https://doi.org/10.1007/s00300-013-1438-x.